Schottky-barrier height and electronic structure of the Si interface with metal silicides: $CoSi_2$, $NiSi_2$, and YSi_2

Hideaki Fujitani
Fujitsu Laboratories Ltd., 10-1 Morinosato-Wakamiya, Atsugi 243-01, Japan

Setsuro Asano
Institute of Physics, College of Arts and Sciences, University of Tokyo, 3-8-1 Komaba, Meguro-ku, Tokyo 153, Japan
(Received 27 December 1993; revised manuscript received 20 April 1994)

Using the linear muffin-tin orbitals in the atomic-sphere approximation with the local-density approximation (LDA), we studied the electronic structure and Schottky-barrier height (SBH) of the Si interface with metal silicides: $CoSi_2$, $NiSi_2$, and YSi_2. We used large supercells with 9 Si_2 and 8–10 silicide ($CoSi_2$, YSi_2) layers for the (111) interface and with 11 Si_2 and 11 silicide ($NiSi_2$, $CoSi_2$) layers for the (001) interface. Together with our previous calculations on the two types of $NiSi_2$/Si(111) interfaces, we demonstrate that the LDA calculation with a large supercell correctly reproduces the dependence of experimental SBH's on the interface structure and type of metal silicide. Electron transfer at the silicide-Si interface depends significantly on the atomic structure of the interface, especially the interfacial space, whether atoms are crowded or not. The energy distribution of interfacial gap states varies significantly with interface atomic structures. These electronic structures directly depend on the interface atomic structure; in contrast, the calculated SBH's do not always depend on the interface structure. We discuss the underlying mechanisms for the formation of Schottky barriers.

I. INTRODUCTION

The interface with silicon (Si) is widely used in microelectronic devices, but its electronic structure is not yet clarified. Since an interface is buried by an overlayer and its structure depends on the materials and conditions used during formation, it is difficult to clarify the atomic structure of the interface. Hence, the electronic structure of real interfaces has not been clarified.

During the last two decades, there was much progress in the *ab initio* self-consistent method for electronic band structures of solids, which is based on the density functional theory.[1] This method has had remarkable success within the local-density approximation (LDA) (Ref. 2) in computing structural, vibrational, and other ground-state properties for a wide range of materials. But it was rarely applied to real interfaces, because the atomic structure of real interfaces is too complicated to study their microscopic characters theoretically. To understand the interface character from the viewpoint of the interface electronic structure, well-defined interfaces are needed and *ab initio* calculations must be employed. Model theories or empirical calculations must always include some assumptions. Since experiments on the interface cannot give unequivocal information about the interface electronic states, the assumption validity cannot be evaluated.

Using LDA calculations, we examined the electronic structures at epitaxial Si interfaces with four different materials: metal silicides ($NiSi_2$, $CoSi_2$, YSi_2) and an insulator (CaF_2). These interfaces have simple atomic structures under some formation conditions and are suitable for studying the electronic structure of real interfaces by *ab initio* calculations. Previously, we gave full descriptions of our calculations for the CaF_2/Si(111) interface[3] and the two types of $NiSi_2$/Si(111) interfaces.[4] As for other interfaces, we made brief reports on our calculations in a Refs. 5–8. In this paper, we give more comprehensive descriptions of our calculations for the $CoSi_2$/Si(111), YSi_2/Si(111), and $NiSi_2$/Si(001) interfaces, including a result with a $CoSi_2$/Si(001) interface. Then, comparing these interfaces, we consider the accuracy of our calculations and the underlying mechanism for the formation of Schottky barriers (SB).

II. PREVIOUS INVESTIGATIONS

Many studies have examined how SB's form at the metal-semiconductor interface.[9–11] It was believed that the material properties, especially those of the semiconductor, determined the Schottky-barrier height (SBH) and that the interface structure does not play an important role in the SB formation.[12–14] However, this understanding was thrown into doubt by Tung's discovery that the SBH at the $NiSi_2$/Si(111) interface depends on the interface atomic structure.[15]

$NiSi_2$ has a fluorite (CaF_2) structure with a lattice constant of 5.406 Å, which is 0.4% smaller than the Si lattice constant of 5.429 Å. $NiSi_2$ epitaxially grown on a Si(111) surface forms an atomically abrupt, structurally perfect interface.[16] This interface has two types of structures. Type-*A* $NiSi_2$ has the same orientation as the Si substrate, and type-*B* $NiSi_2$ is rotated 180° about the

Si⟨111⟩ axis. In 1984, Tung discovered that the SBH of the two types of interfaces differ by 0.14 eV. The n-type SBH [the conduction band minimum (E_c) minus the Fermi level (E_f)] is 0.65 eV for the type-A interface and 0.79 eV for the type-B interface.

Using the linear muffin-tin orbitals in the atomic-sphere approximation (LMTO-ASA), we got different SBH's for the two types of $NiSi_2$/Si(111) interface, which is consistent with Tung's work.[17] Shortly after our work, Das *et al.* reported similar results that agreed qualitatively with ours, but differed quantitatively.[18] We performed further calculations with different conditions to resolve the discrepancy.[4] The $NiSi_2$/Si(111) interface is the first example of a real metal-semiconductor interface whose atomic structure has been clarified and for which reliable *ab initio* calculations were performed. To further investigate the dependence of SBH on the interface atomic structure, other examples must be examined.

$CoSi_2$ also has a fluorite structure and a lattice constant 5.356 Å, which is 1.3% smaller than that of Si. Epitaxial $CoSi_2$ film can be grown by the deposition and annealing of Co on a Si(111) surface. This primarily forms a type-B interface. Lattice images obtained by transmission electron microscopy (TEM),[19,20] x-ray standing wave (XSW) measurements,[21] and Rutherford backscattering,[22] suggested that the interfacial Co atom was fivefold coordinated. Hamann showed by linear augmented plane wave (LAPW) calculations, however, that the structure with eightfold-coordinated interfacial Co atoms has the lowest energy and that the fivefold structure is extremely unfavorable.[23] Hamann pointed out that none of the experiments can rule out the eightfold structure at the $CoSi_2$/Si(111) interface (Fig. 1).

Rees and Matthai studied the type-B $CoSi_2$/Si(111) interface using a tight-binding method with the extended Hückel approximation.[24] They reported that the n-type SBH is 0.55 eV for the fivefold interface and 0.13 eV for the eightfold interface. Using LMTO-ASA calculations, however, we obtained different SBH's at the $CoSi_2$/Si(111) interface. We showed that the fivefold $CoSi_2$/Si(111) interface gives an unreasonable negative p-type SBH: the Fermi level (E_f) is lower than the valence band maximum of Si (E_v), while the eightfold interface gives a positive and reasonable SBH.[6] The density of states (DOS) of bulk Si and $CoSi_2$ obtained with the extended Hückel approximation differ significantly from the DOS obtained by more accurate methods [pseudopotential[25] and full-potential LAPW (Ref. 26)]. Hence, the extended Hückel approximation does not accurately describe the electronic structure at the silicide/Si interface.

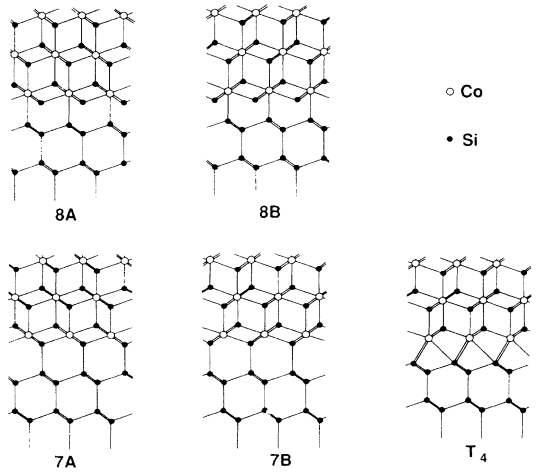

FIG. 1. Atomic structure at $CoSi_2$/Si(111) interface: eightfold type-A ($8A$), eightfold type-B ($8B$), sevenfold type-A ($7A$), and sevenfold type-B ($7B$), T_4 site type-B models (T_4).

Although most structure probes cannot access the buried interface, surface structures often indicate the interface atomic structure. Hellman and Tung discovered that two distinctly different surface structures can be formed on a $CoSi_2$(111) surface.[27] One has a bulk termination of the $CoSi_2$ lattice. The other has bulk-Si-like double layers on the $CoSi_2$(111) surface, which gives eightfold coordination to the surface Co atoms. Subsequently, many experimental methods were used to distinguish between fivefold- and eightfold-coordinated interfacial Co atoms: medium-energy ion scattering,[28,29] surface extended x-ray absorption fine-structure analysis,[30] and angle-resolved photoemission.[31] These techniques supported the eightfold coordination of the interfacial Co atoms.

Compared to the $NiSi_2$/Si(111) interface, the $CoSi_2$/Si(111) interface structure is more complicated, partly because $CoSi_2$ has a slightly larger lattice mismatch with Si. Although the type-B eightfold structure is energetically more favorable than the type-A interface,[23] a type-A structure can be formed at the $CoSi_2$/Si(111) interface.[32,33] For the type-B $CoSi_2$/Si(111) interface, evidence for more than one quasistable atomic structure has been observed, including high-resolution electron microscopy images which suggest a sevenfold structure.[34,35] Fully annealed $CoSi_2$ films with a high density of misfit dislocations usually have a SBH between 0.65 eV and 0.70 eV on n-type Si(111).[36,37] At a type-B interface with a low dislocation density formed by repeated deposition and annealing over thin templates, the n-type SBH varies from about 0.5 eV to 0.7 eV.[35]

In 1993, by carefully controlled molecular beam epitaxy, Sullivan *et al.* grew single-crystal type-B $CoSi_2$/Si(111) interfaces with a giant variation in SBH's.[38] One interface, probably with the eightfold structure, had an n-type SBH of 0.69 eV. But, other interfaces had an n-type SBH of 0.27 eV, which was fabricated with a sandwich structure prepared by depositing 7 Å of Co, then 25 Å of Si at room temperature, and was annealed at 500 °C for 10 min. Slight deviation in this recipe, either film stoichiometry or annealing temperature, produced interfaces with an intermediate SBH.

Rare-earth silicides are unique in that they have an n-type SBH (0.37–0.39 eV) lower than half the Si band gap,[39] while most metals have a SBH higher than half the Si band gap. YSi_2 is a layered rare-earth silicide. It has a $C32$ crystal structure (AlB_2 type) with a hexagonal unit

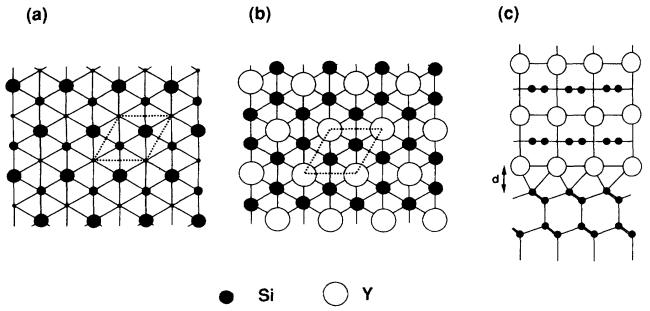

FIG. 2. (a) Overview of unrelaxed Si(111) surface, (b) overview of YSi_2 surface, and (c) cross section at YSi_2/Si(111) interface.

cell whose lattice constants are 3.842 Å for the a axis and 4.144 Å for the c axis.[40] Within each Si layer, atoms are arranged in a planar mesh with sixfold symmetry. $YSi_{1.7}$ has a defective AlB_2 structure and one Si atom in six is missing. YSi_{2-x} ($x = 0$ and $x = 0.3$) has a lattice mismatch only 0.1% relative to the Si(111) surface lattice, hence it is possible to grow large, perfect YSi_{2-x} silicide films on Si(111).[40,41] Each film stoichiometry depends on the formation conditions. The interface atomic structure has not yet been clarified, but the surface structure of YSi_2 suggests the interface atomic structure. Baptist *et al.* reported that the YSi_2 surface is Si terminated and every other Si atom is displaced 0.8 Å upward. Hence, the surface geometry is the same as that of a 1×1 Si(111) surface.[42] This suggests that the top Si layer of YSi_2 continues to the Si substrate at the interface and the interfacial Y atoms reside at H_3 sites (Fig. 2).

A $NiSi_2$/Si(001) interface usually has an n-type SBH of 0.65 eV, which is the same as the SBH of the (111) type-A interface. TEM lattice images show that the $NiSi_2$/Si(001) interface has a sixfold structure in which the interface Ni atoms are sixfold coordinated (Fig. 3).[43] $NiSi_2$/Si(001) interfaces formed by the conventional template technique, however, contain many dislocations and ⟨111⟩ facets. Thus, the observed SBH at the $NiSi_2$/Si(001) interface was attributed to the (111) facets. In 1991, Tung *et al.* fabricated a single-crystal, uniform, planar $NiSi_2$/Si(001) interface by depositing stoichiometric $NiSi_2$ on Si(001) at low temperatures and annealing at high temperatures (>700 °C).[44] This interface has a low n-type SBH of about 0.4 eV Together with the two types of (111) interfaces, the SBH at the $NiSi_2$/Si interface differs by about 0.4 eV in the same way as at the type-B $CoSi_2$/Si(111) interfaces.

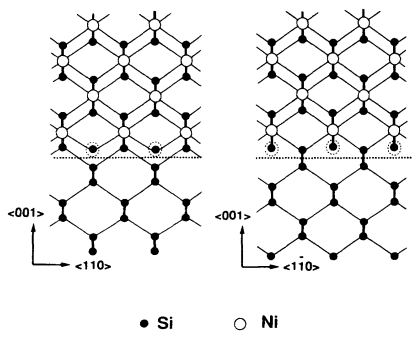

FIG. 3. Atomic structure at the $NiSi_2$/Si(001) interface. With atoms surrounded by dotted circles the interface has eightfold structure.

III. CALCULATIONS

We used scalar relativistic LMTO-ASA for calculations with large supercells. Exchange and correlation are determined by LDA with the parametrization of Janak, Moruzzi, and Williams.[45] We used a nearly orthogonal representation for the muffin-tin orbitals and did not include the combined correction.[46] The LMTO method is the linearized version of the Korringa-Kohn-Rostoker method. It provides almost the same accuracy as full-potential LAPW (FLAPW) for many materials,[47] and computationally it is the fastest of the band calculation methods.

The LMTO-ASA divides the region of space into overlapping Wigner-Seitz spheres which may contain the nuclei. Spheres that do not contain nuclei are known as "empty spheres." In the LMTO-ASA, the sphere radii affect both the band dispersion and total energy, while in FLAPW they only specify a linear basis set detail. Hence, the sphere radii must be more carefully chosen for the LMTO-ASA than FLAPW. We determined the atomic-sphere radii for the band dispersion of bulk occupied states to agree with that given by the FLAPW calculations.

$CoSi_2$ has the same fluorite structure as $NiSi_2$. Although Co atoms have one less d electron than Ni atoms, $CoSi_2$ has an electronic structure similar to that of $NiSi_2$.[26] We used the same atomic-sphere radii for $NiSi_2$ and $CoSi_2$ to accurately compare the interface electronic structure. YSi_2 has a $C32$ crystal structure and does not contain empty spheres. For the LMTO-ASA, the total volume of spheres must equal the unit cell volume. Choosing the Si radius in YSi_2 automatically determines the Y radius. When the Si radius in YSi_2 is set to that of bulk Si, the LMTO calculations agree well with FLAPW result (see Sec. IV B). Hence, we used these radii in calculations for the YSi_2/Si(111) interface. Table I lists the

TABLE I. Atomic-sphere radii and number of electrons in bulk calculations.

Material	Atomic sphere	Sphere radii (Å)	Number of electrons
Si	Si	1.337	13.212
	emp	1.336	0.788
$NiSi_2$	Ni	1.222	27.730
	Si	1.337	13.218
	emp	1.433	1.833
$CoSi_2$	Co	1.222	26.679
	Si	1.337	13.232
	emp	1.433	1.857
YSi_2	Y	1.991	40.324
	Si	1.337	13.338

atomic-sphere radii and number of electrons for the bulk calculations. We used nine muffin-tin orbitals of s-, p-, and d-. For Y atoms we included additional f orbitals. The bulk band gap calculated by the LMTO-ASA for Si was 0.55 eV, although the measured band gap is 1.12 eV. Despite this discrepancy, the calculated SBH correctly reflects the difference of silicide and the interface structure.

The lattice mismatch between Si and these silicides is very small. Although XSW measurements suggest that the Si-Si bond length at the interface is longer in type-A $NiSi_2$/Si(111) than in type-B,[48] conflicting results have been reported.[49] The detailed atomic structure of these interfaces has not been determined. We neglected lattice relaxation and used the Si lattice constant of 5.429 Å to decide the atom positions in the supercell. Since a supercell has two interfaces with the same atomic structure, it is symmetrical. The supercell must be large enough for the central region between the interfaces to be considered bulklike. We previously examined the two types of $NiSi_2$/Si(111) interfaces, and used four supercells with m $NiSi_2$ layers and n Si_2 layers: $m/n = 2/3, 5/6, 8/9$, and $11/12$. All these supercells have a space-group symmetry of $P\bar{3}m1$ (D_{3d}^3). We found that the 8/9 supercell is almost large enough to examine the interface electronic structure. Hence, for other (111) interfaces, we used the supercells with the $P\bar{3}m1$ symmetry and nine Si_2 layers. We chose the number of silicide layers to maintain the space-group symmetry. For (001) interfaces of $NiSi_2$/Si and $CoSi_2$/Si, we used supercells with a space-group symmetry of $Cmmm$ (D_{2h}^{19}). Table II lists the interface structures and supercell sizes for which we carried out the LMTO-ASA calculations.

Since an interface is formed by two materials, an interstitial space at the interface depends on the atomic structure. We put empty spheres into the interstitial space so that the total volume of spheres equaled the supercell volume. When one empty sphere enters at the interface, its radius is automatically determined. When two empty spheres enter, their radii are not uniquely determined, although the bulk atomic-sphere radii are determined to agree with FLAPW. We determined positions and radii of the interfacial empty sphere needed to fill the interfacial space and decrease the overlap between neighboring spheres. This rule worked well for all the supercells in Table II except the $8B$ $CoSi_2$/Si(111) interface, where it makes the radius of the interfacial empty sphere too large, and the empty sphere overlaps excessively with the neighboring spheres. To reduce the interfacial empty sphere's radius, we enlarged the radius of the first empty sphere on the Si side.

TABLE II. Supercell size for interfaces.

Interfaces	Structure	Supercell size
$CoSi_2$/Si(111)	$8A$	$10(CoSi_2)/9(Si_2)$
	$8B$	$10(CoSi_2)/9(Si_2)$
	$7A$	$8(CoSi_2)/9(Si_2)$
	$7B$	$8(CoSi_2)/9(Si_2)$
	T_4	$6(CoSi_2)2(CoSi)/9(Si_2)$
YSi_2/Si(111)	H_3	$10(YSi_2)/9(Si_2)$
$NiSi_2$/Si(001)	sixfold	$5(NiSi_2)2(NiSi)/7(Si_2)$
	eightfold	$11(NiSi_2)/11(Si_2)$
$CoSi_2$/Si(001)	eightfold	$11(CoSi_2)/11(Si_2)$

To get an accurate self-consistent potential for these large supercells, we first considered a smaller supercell, for example, a 5/6 supercell. We used the small supercell's self-consistent potential as the initial potential for a larger supercell. First, we did self-consistent iterations with 9 to 25 nonequivalent $\mathbf{k}$ points in the supercell's first Brillouin zone. To get the final self-consistent potential, we used from 81 to 100 nonequivalent $\mathbf{k}$ points.

IV. RESULTS

A. $CoSi_2$/Si(111) interface

1. *Type-A and -B eightfold structures*

For the LMTO-ASA calculation, the local density of states (LDOS) in the i atomic or empty sphere is given by

$$N_i(E) = \sum_{\mathbf{k}_{||},n} \int_{\Omega_i} |\psi_{\mathbf{k}_{||},n}(\mathbf{r})|^2 d^3r \delta[E - E_n(\mathbf{k}_{||})], \quad (1)$$

where $\mathbf{k}_{||}$ is the wave vector parallel to the interface, n is the band index, $\psi_{\mathbf{k}_{||},n}$ is the wave function, and Ω_i is the volume of the i sphere.

Figure 4 shows the LDOS of the eightfold $CoSi_2$/Si(111) interfaces, which are now believed to be the correct interface structure. The first Si_2 layer's LDOS differs significantly from the bulk Si DOS (dotted lines) because it has an eightfold-coordinated interfacial Co atom and a Co-Si bond forms at the interface (Fig. 1). The peak at -4 eV in the bulk $CoSi_2$ DOS is evidence of Co-Si bond which consists of Si p and Co d orbitals. In the first Si_2 layer, the DOS peaks slightly at -4 eV.

An interfacial Si atom has an imperfect tetrahedral structure and one dangling bond, which is the origin of interface states (shaded areas in Fig. 4). The interface states in the Si band gap are formed mainly by Si p orbitals, and those at the bottom of the valence band are formed by Si s orbitals. In the first $CoSi_2$ layer, the two types of interface have slightly different peaks just above the Fermi level (shaded areas). The type-B interface has a slightly sharper and higher peak than the type-A; dangling bond character remains stronger at the type-B interface. Since the interfacial atomic structure directly affects the interface states, structural differences between the two types of interfaces cause the different peaks. At the type-A interface, the distance between the interfacial Si atom and the second Si atom in the Si layer is the same as the bulk Si-Si distance. The bonding interaction between these atoms is stronger at the type-A interface than at the type-B interface.

Hamann did full-potential LAPW calculations for the $CoSi_2$/Si(111) interfaces with 2/2 supercells and plotted the interface electron density.[23] The contour plot of the type-A interface's electron density contains extra con-

tours between the interfacial Si atom and the second Si atom in the first Si_2 layer, but the type-B interface's plot does not. The second Si atoms of the type-A interface are overcoordinated. Since the small peak caused by the dangling bond is broader for the type-A interface, our LDOS is consistent with Hamann's electron density plot.

We examined the wave function weights of the energy eigenvalues of the 10/9 supercell in each atomic sphere of the Si and $CoSi_2$ layers. From this, we drew a schematic two-dimensional band structure along the symmetry lines of the type-A $CoSi_2$/Si(111) interface (Fig. 5). The zero energy is the supercell's Fermi level (E_f). Bold lines in Fig. 5 are interface states for which more than 40% of wave functions are in the four atomic spheres (three Si and one Co sphere) at the interface. The interface state indicated by the upper line in the Si band gap is formed mainly by Si p orbitals, and the lower line is formed mainly by Si p orbitals with a few Co d orbitals. The upper line corresponds to the shaded area in the Si band gap in Fig. 4(a). The interface states indicated by the lower line cause a small peak in the LDOS [indicated by an arrow in Fig. 4(a)]. The interface states around -4 eV correspond to the interfacial Co-Si bond.

The energy states in the Si band gap are classified into two categories. One category is interface states whose wave functions are localized near the interface and decay on both sides of the interface. The other category is metal-induced gap states (MIGS's) whose wave functions decay only on the semiconductor side. Interface states originate in the interfacial bond configuration, and

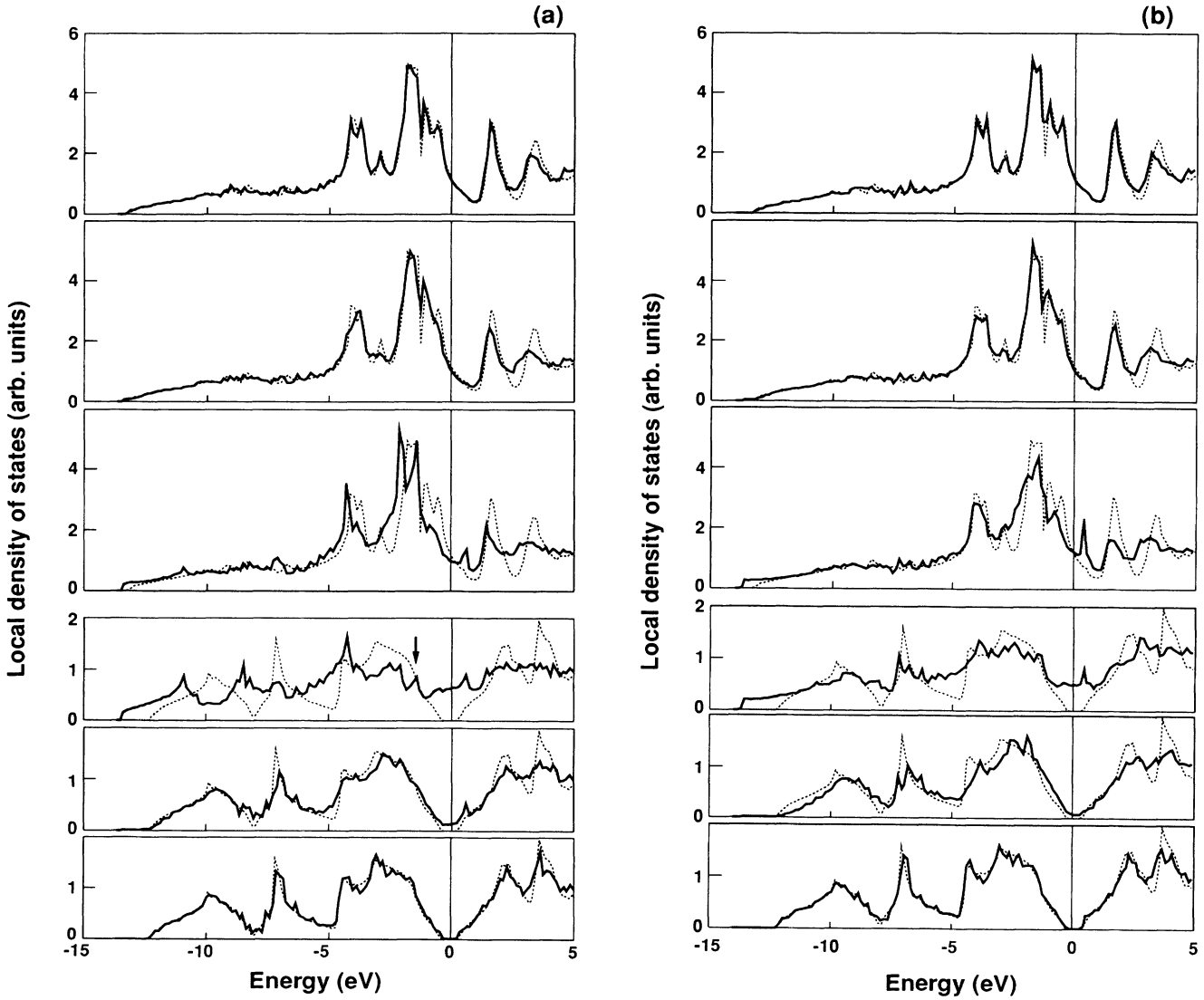

FIG. 4. Local densities of states at the (a) type-A and (b) type-B eightfold $CoSi_2$/Si(111) interfaces. From top to bottom are the $CoSi_2$ layer furthest from the interface, the second $CoSi_2$ layer, the first $CoSi_2$ layer, the first Si_2 layer, the second Si_2 layer, and the Si_2 layer furthest from the interface. Dotted lines are bulk densities of states of Si and $CoSi_2$. Shaded areas are interface states. The zero energy point is the Fermi energy of the supercell.

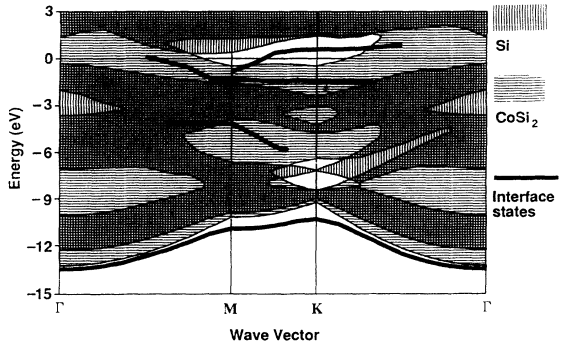

FIG. 5. Two-dimensional projected band structure of the type-A $CoSi_2$/Si(111) interface obtained from the supercell calculation. The zero energy point is the Fermi energy. Bold lines indicate the interface states that are localized near the interface.

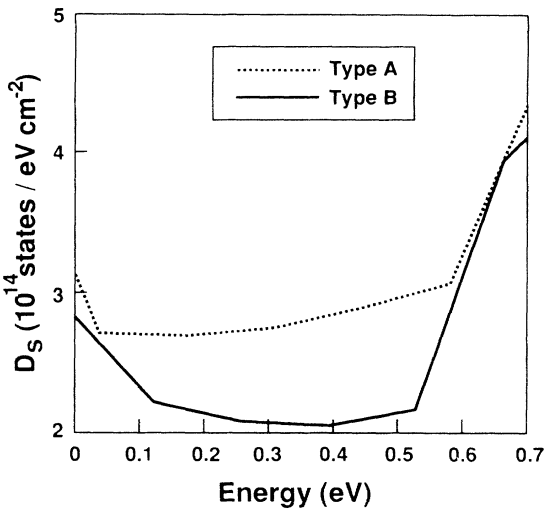

FIG. 6. Surface densities of interfacial states in the Si band gap at the two types of eightfold $CoSi_2$/Si(111) interfaces.

sometimes overlap the projected bulk band of the metal or semiconductor. MIGS's form only in the energy region where the bulk band of the metal is projected. Since the two-dimensional energy structure of metal depends on the interface orientation, MIGS's depend on the projected metal band structure at the homogeneous metal-semiconductor interface.

The projected band structure (Fig. 5) shows that the interface states in the Si band gap disappear near the Γ point. When the interface states overlap the bulk band, their wave functions may extend into the metal or semiconductor layers, depending on the $\mathbf{k}$ point. Since this delocalization of the wave function occurs gradually, we cannot clearly distinguish between MIGS's and the interface states. We call the mixture of MIGS's and interface states "interfacial gap states."

The Si layer band gaps obtained from the eigenvalues of the 10/9 supercells were 0.71 eV for the type-A and 0.70 eV for the type-B $CoSi_2$/Si(111) interfaces. We obtained the surface density of the gap states (D_s) by summing the LDOS between E_v and E_c of the all spheres in the Si layer (Fig. 6). As with gap states at the $NiSi_2$/Si(111), gap states at the $CoSi_2$/Si(111) are mainly formed by Si p orbitals and are concentrated in the Si spheres rather than in the interstitial empty spheres (Fig. 8 in Ref. 4).

The origin of the interface states in the Si band gap is the interfacial Si atom's dangling bond at the eightfold $CoSi_2$/Si(111) interfaces and the interfacial Ni atom's dangling d orbital at the sevenfold $NiSi_2$/Si(111) interfaces. Since the interfacial gap states are formed mainly by Si p orbitals in the Si layer, the Si dangling bond's wave function extends more easily into the Si layer than that of the dangling d orbital. This is why the D_s of the $CoSi_2$/Si(111) is higher than that of $NiSi_2$/Si(111) (Fig. 7 in Ref. 4).

We compared number of electrons in the spheres at the type-A eightfold $CoSi_2$/Si(111) interface with the bulk values (Table I and Fig. 7). In this structure, one empty sphere enters at the interface. It has a 1.386 Å radius and contains 1.448 electrons. In both the Si and the $CoSi_2$ layers, spheres close to the interface have more electrons than the bulk. In the Si layer, the first and second Si spheres have more electrons and the third Si sphere has less electrons than the bulk. The second Si sphere has to contain many electrons because of the extra bond between the interfacial Si atom and the second Si atom. Since the third Si sphere has less electrons, there are probably less electrons between the second and third Si atoms. In the $CoSi_2$ layer, the first Si-Co-Si spheres have more electrons than the bulk. From the contour plot of the interfacial electron density, Hamann found that the Co-Si bonds in the $CoSi_2$ layer were stronger than those in the bulk and the bonds in the Si layer were weaker.[23] Figure 7 is consistent with Hamann's result.

For the sevenfold $NiSi_2$/Si(111) interfaces, unlike the eightfold $CoSi_2$/Si(111) interface, atomic spheres close to the interface have less electrons than the bulk (Fig. 4 in Ref. 4). Two empty spheres enter at the sevenfold $NiSi_2$/Si(111) interface, but one empty sphere enters at the eightfold $CoSi_2$/Si(111) interface. In the sevenfold structure electron transfer occurs to fill the large interfacial space. But the eightfold structure has less interfacial space: atoms are crowded at the interface. Hence, electrons overflow at the eightfold $CoSi_2$/Si(111) interface and spheres close to the interface have more electrons. The interfacial space significantly affects the electron distribution at the silicide/Si interface.

At the type-B eightfold $CoSi_2$/Si(111) interface, we enlarged the radius of the first empty sphere on the Si side to reduce the interfacial empty sphere's radius. In the ASA calculations, since neighboring atomic spheres overlap, the spheres must have the same radius to compare the number of electrons in spheres. Therefore, at the type-B eightfold $CoSi_2$/Si(111) interface, only the outline of the electron distribution can be compared with the bulk. Table III lists the number of electrons of the type-B eightfold $CoSi_2$/Si(111) interface. The interfacial

TABLE III. Number of electrons in the spheres near the eightfold type-B $CoSi_2$/Si(111) interface. The radius of the first empty sphere in the Si layer (a) is 1.529 Å, which is larger than the radius of other empty spheres in the Si layer.

	Si layer		$CoSi_2$ layer	
	Sphere	Electrons	Sphere	Electrons
1	Si	13.451	Si	13.417
2	Si	13.063	Co	26.742
3	emp[a]	1.414	Si	13.245
4	emp	0.699	emp	1.846
5	Si	13.065	Si	13.221
6	Si	13.155	Co	26.682
7	emp	0.796	Si	13.234
8	emp	0.802	emp	1.856
9	Si	13.215	Si	13.231
10	Si	13.210	Co	26.681

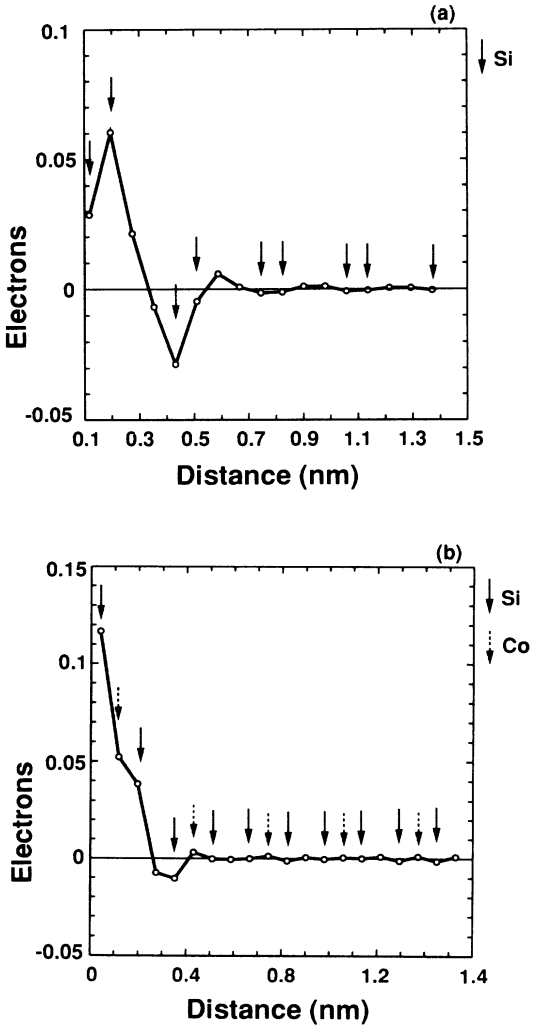

FIG. 7. Difference in the number of electrons in the spheres from the bulk values at the type-A eightfold $CoSi_2$/Si(111) interface: (a) in the Si layer and (b) in the $CoSi_2$ layer. The interface is on the left-hand side. Arrows indicate atomic-sphere locations.

empty sphere has a radius of 1.137 Å and contains 1.027 electrons (not listed in Table III). In the $CoSi_2$ layer of the type-B interface, the first $CoSi_2$ spheres have more electrons than the bulk, as with the type-A interface. In the Si layer, the first Si sphere has more electrons and the total number of electrons in the next Si-emp-emp-Si spheres is larger than in the bulk. Hence, because atoms are crowded at the interface, electrons overflow on both sides of the type-B interface in the same way as at the type-A interface.

2. *Type-A and -B sevenfold structures*

We studied sevenfold $CoSi_2$/Si(111) interfaces that have the same structure as the type-A and -B $NiSi_2$/Si(111) interfaces. Since the radii and positions of the atomic and empty spheres are the same as those of the $NiSi_2$/Si(111) interfaces, the calculations are under the same conditions. Only the metal atom differs; Co atoms have one less d electron than Ni atoms.

The LDOS of the sevenfold $CoSi_2$/Si(111) interface (Fig. 8) resembles that of the $NiSi_2$/Si(111) interface (Fig. 2 in Ref. 4). In the Si layers near the interface, the sharp peak at −7 eV and the small dip at 3 eV disappear like the $NiSi_2$/Si(111) interface. The interface states are also formed in the Si band gap. They consist mainly of the interfacial Co atom's d orbitals and of Si p orbitals in the Si layers. The interface state energy is a little higher than that of the $NiSi_2$/Si(111) interfaces because the Co d orbital has a higher energy; the large d-electron peak of $CoSi_2$ is at a higher energy than that of $NiSi_2$. The partial band gap of $CoSi_2$ that appears in the (111) projected two-dimensional Brillouin zone is also at a higher energy than that of $NiSi_2$ (Fig. 5 in Ref. 4). In the $CoSi_2$ layers near the interface, the large d-electron peak is shifted to a slightly higher energy. This shift occurs at the $NiSi_2$/Si(111) interfaces, although it is smaller in the $CoSi_2$/Si(111) than in the $NiSi_2$/Si(111).

The difference in number of electrons from the bulk value (Table I) is almost the same between the sevenfold $CoSi_2$/Si(111) (Fig. 9) and the $NiSi_2$/Si(111) for each type of interface (Fig. 4 in Ref. 4). Table IV lists the sphere radii and number of electrons of interfacial empty spheres (not shown in Fig. 9). The total number of electrons in the two empty spheres is 0.015 larger than that of the $NiSi_2$/Si(111) interface for each type of interface. Hence, the number of electrons in the spheres close to the $CoSi_2$/Si(111) interface is slightly less than in the spheres close to the $NiSi_2$/Si(111) interface. This is reasonable because bulk $CoSi_2$ has 0.024 more electrons in the empty sphere than bulk $NiSi_2$ (Table I).

TABLE IV. Atomic-sphere radii and number of electrons in the empty spheres located at the sevenfold $CoSi_2$/Si(111) interfaces.

	Type-A		Type-B	
Sphere radius (Å)	1.389	1.334	0.971	1.612
Number of electrons	1.120	0.777	0.312	1.648

Compared with the electron distribution at the eightfold $CoSi_2$/Si(111) interface (Fig. 7), the sevenfold $CoSi_2$ and $NiSi_2$ interfaces have similar distributions. The electron distribution at the silicide/Si interface is determined by the interfacial atomic structure, especially the volume of the interfacial space.

Using LMTO-ASA, it is difficult to study the dependence of the total energy on the interface structure. We can, however, compare the interface energies of sevenfold interfaces of the same type, because the position and radii of the atomic spheres for each type of $CoSi_2$/Si(111) and $NiSi_2$/Si(111) interface are the same. The interface energy is defined as half the supercell energy minus half the sum of the energy of a number of unit cells of each bulk material. The interface energy is higher at the sevenfold $CoSi_2$/Si(111) interface than at the sevenfold $NiSi_2$/Si(111) interface; 0.55 eV higher for the type-A interface and 0.64 eV higher for the type-B interface. From full-potential LAPW calculations, Hamann obtained a $CoSi_2$/Si(111) interface energy 0.51 eV higher than the $NiSi_2$/Si(111) interface for the type-A sevenfold structure.[23] This agrees well with our results, although we used a supercell size of 8/9 and Hamann used 2/2.

3. *The T_4 structure*

To examine the possible interface structure with a high p-type SBH, we took the type-B $CoSi_2$/Si(111) interface structure, whose interfacial Co atom is at the T_4 site,

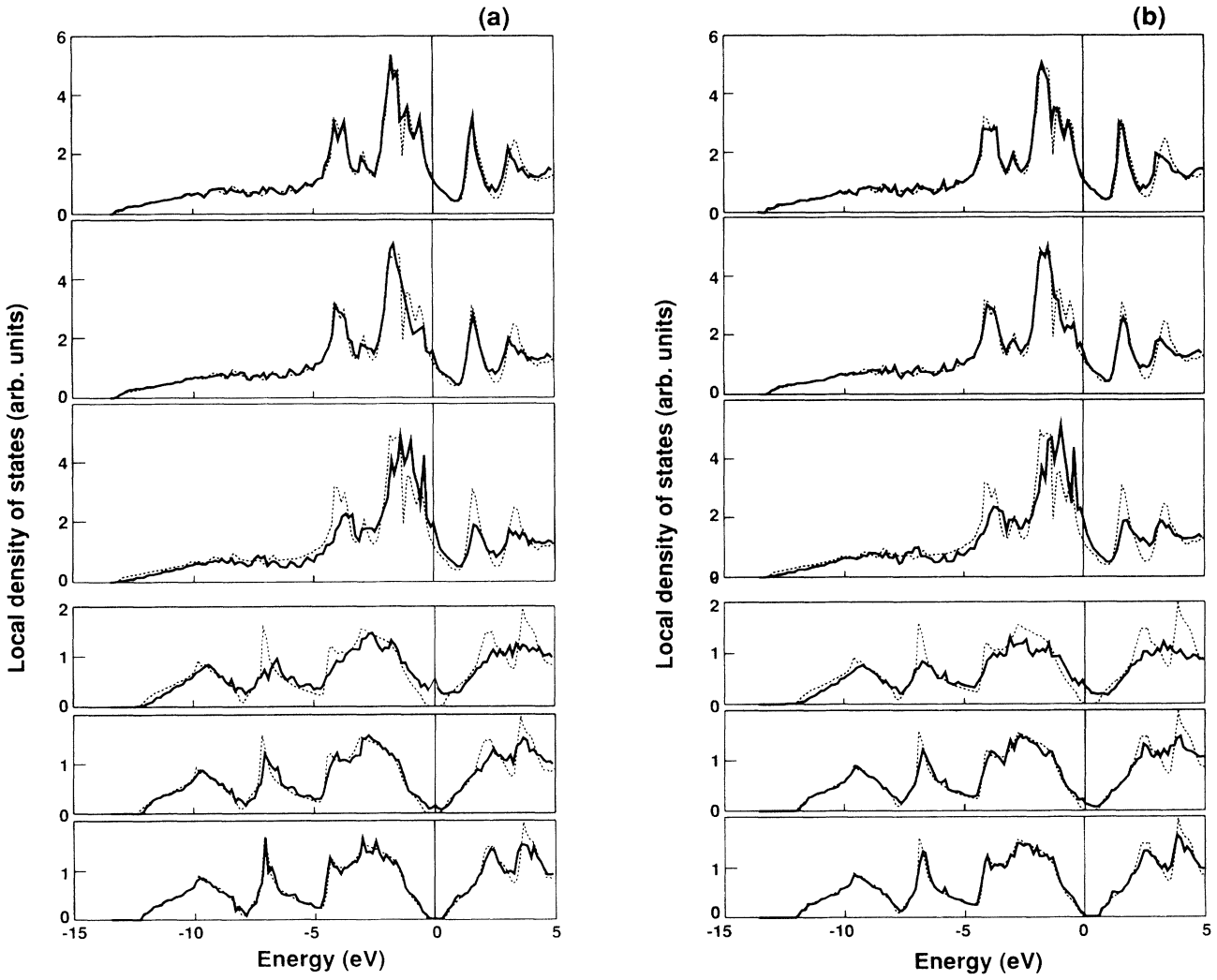

FIG. 8. Local densities of states at the (a) type-A and (b) type-B sevenfold $CoSi_2$/Si(111) interfaces. From top to bottom are the $CoSi_2$ layer furthest from the interface, the second $CoSi_2$ layer, the first $CoSi_2$ layer, the first Si_2 layer, the second Si_2 layer, and the Si_2 layer furthest from the interface. Dotted lines are bulk densities of states of Si and $CoSi_2$. Shaded areas are interface states. The zero energy point is the Fermi energy of the supercell.

from the CaF_2/Si(111) interface.[3] We set the distance between the interfacial Co layer and the first Si layer to 2.037 Å. The interface states in the Si band gap have two bonding and antibonding peaks, because they originate from the bonding interaction between the interfacial Co and Si atoms (Fig. 10). In the Si layer, the interface bonding states are formed by Si p orbitals and the antibonding states are formed by Si s and p orbitals. In the first $CoSi_2$ layer, the interface states (shaded area) are formed mainly by Co d orbitals.

In both eightfold and sevenfold structures, the interfacial Si atom on the Si side is tetrahedrically bonded to its four nearest neighbors, even though the interfacial atom on the silicide side has a dangling bond. In the T_4 structure, the interfacial Si atom on the Si side is bonded to the three nearest Si atoms (back bonds). The interfacial Co-Si bonding interaction and the back bonds of the interfacial Si atom are in the same direction in the interface plane. Like bulk $CoSi_2$, the interfacial Co atom has eightfold coordinations.

We compared numbers of electrons in the spheres at the T_4 $CoSi_2$/Si(111) interface with the bulk value (Table I, Fig. 11). Table V lists the radii and number of electrons of two empty spheres at the interface. The number of electrons decays on both sides of the interface. In the sevenfold structure (Fig. 9), the sphere closest to the interface has a maximum of 0.2 less electrons. In the T_4 structure, the interfacial Si sphere on the Si side has about 0.3 less electrons and the interfacial Co sphere has about 0.5 less electrons than the bulk. Compared with the $NiSi_2$/Si(111) interfaces and the eightfold and sevenfold $CoSi_2$/Si(111) interfaces (Figs. 7 and 9), the difference at the T_4 interface is very large. In bulk $CoSi_2$ and $NiSi_2$, Si atoms supply many electrons in the empty sphere (Table I). The T_4 structure has a Co-Si

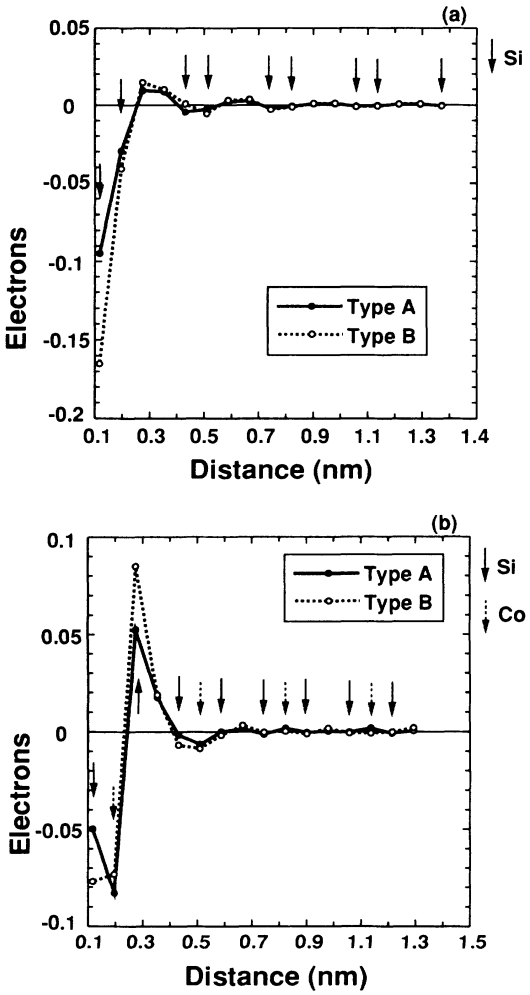

FIG. 9. Difference in the number of electrons in the spheres from the bulk values at the sevenfold $CoSi_2$/Si(111) interfaces (a) in the Si layer and (b) in the $CoSi_2$ layer. The interface is on the left-hand side. Arrows indicate atomic-sphere locations.

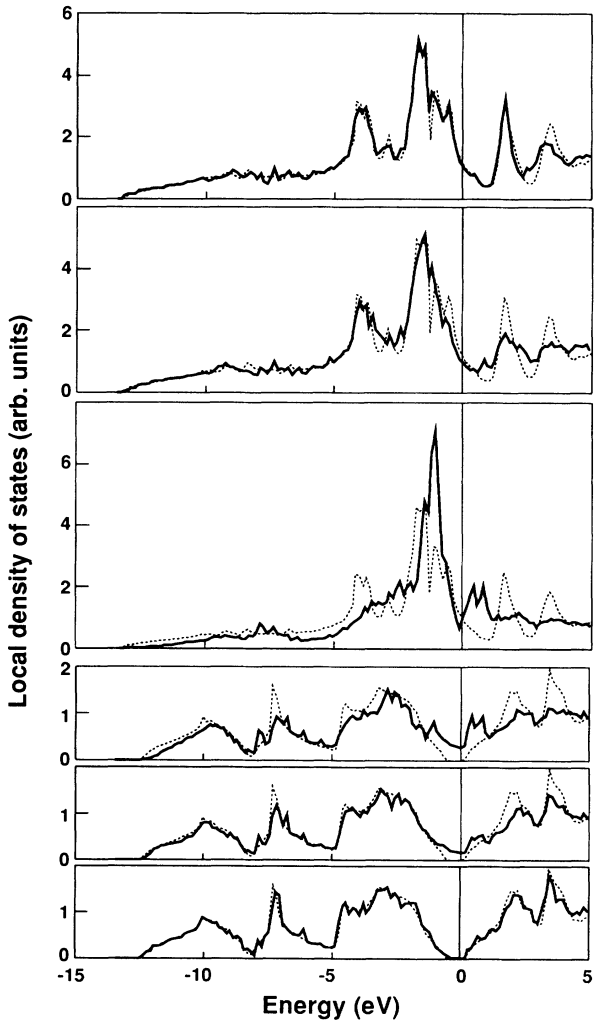

FIG. 10. Local density of states of the type-B $CoSi_2$/Si(111) interface whose interfacial Co atom is at the T_4 site. From top to bottom are the $CoSi_2$ layer furthest from the interface, the second $CoSi_2$ layer, the first CoSi layer, the first Si_2 layer, the second Si_2 layer, and the Si_2 layer furthest from the interface. Dotted lines are bulk densities of states of Si and $CoSi_2$. Shaded areas are interface states. The zero energy point is the Fermi energy of the supercell.

TABLE V. Atomic-sphere radii and number of electrons in the empty spheres located at the T_4 $CoSi_2$/Si(111) interface.

Sphere radius (Å)	1.036	1.440
Number of electrons	0.548	1.449

layer at the interface, while the sevenfold and eightfold structures have a Si-Co-Si layer at the interface. The T_4 structure lacks one Si layer between the interfacial empty sphere layer and the first empty sphere layer on the $CoSi_2$ side. This is why the T_4 structure has far fewer electrons even though the total volume of the two interfacial empty spheres is slightly larger in the sevenfold structure than in the T_4 structure (Tables IV and V).

4. SBH at the $CoSi_2$/Si(111) interface

Table VI lists calculated SBH's ($E_f - E_v$) at the $CoSi_2$/Si(111) interface. These were obtained from the

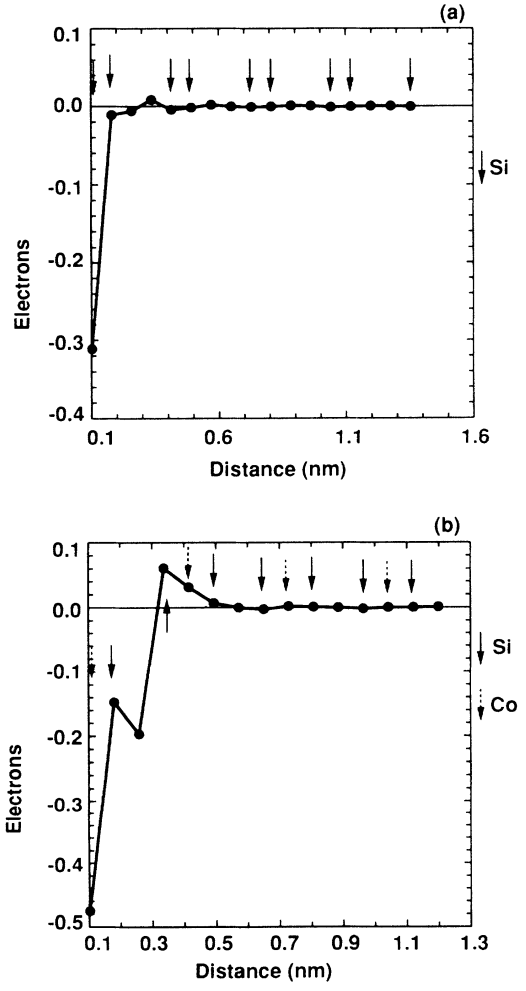

FIG. 11. Difference in the number of electrons in the spheres from the bulk values at the type-B $CoSi_2$/Si(111) interface whose interfacial Co atom is at the T_4 site, (a) in the Si layer and (b) in the $CoSi_2$ layer. The interface is on the left-hand side. Arrows indicate atomic-sphere locations.

TABLE VI. Calculated Schottky-barrier height ($E_f - E_v$) at the $CoSi_2$/Si(111) interfaces obtained from the eigenvalue of the supercell and by the frozen potential method (in eV).

Structure	By eigenvalue	By frozen potential
$8A$	0.37	0.29
$8B$	0.25	0.19
$7A$	0.29	0.24
$7B$	0.07	−0.01
T_4	0.49	0.42

supercell's eigenvalue and Fermi energy, or by the frozen potential method (see Sec. V A). The p-type SBH at the metal-semiconductor interface is

$$\Phi_{Bp} = \chi_s + E_g - \phi_m + D_0, \tag{2}$$

where ϕ_m is the metal work function, E_g and χ_s are the band gap and electron affinity in the semiconductor, and D_0 is the electrostatic interface dipole, which is determined by the electron distribution at the interface.[50] When only the interface structure varies, χ_s, E_g, and ϕ_m are constant and only the interfacial dipole (D_0) can differ. The type-A eightfold and sevenfold $CoSi_2$/Si(111) interfaces have very different electron distributions but their SBH's differ by only 0.08 eV. The type-A and -B sevenfold interfaces have similar electron distributions, but their SBH's differ by 0.22 eV. The electron distribution difference does not correspond to the SBH difference. When atoms are crowded at the interface, as in the eightfold structure, electrons overflow. When the interfacial space is large, as in the sevenfold and T_4 structures, the spheres close to the interface have less electrons than the bulk. At the silicide/Si interface, a large part of electron transfer occurs to neutralize the charge distribution caused by the interface atomic structure, especially by the interfacial space. This electron transfer is independent of the SBH, that is, the interfacial dipole (D_0).

The experimental p-type SBH of 0.43 eV for the $CoSi_2$/Si(111) interface that probably has an eightfold structure[38] lies between the SBH's at the two types of $NiSi_2$/Si(111) interfaces. The calculated SBH of 0.25 eV for the type-B eightfold $CoSi_2$/Si(111) interface also lies almost between the SBH's calculated for the $NiSi_2$/Si(111) interface using a supercell with nine Si_2 layers. Sullivan *et al.* reported an extremely high p-type SBH for the type-B $CoSi_2$/Si(111) interface. The calculated SBH for the type-B sevenfold interface is 0.07 eV, which is smaller than that of the type-B eightfold interface. Hence, the sevenfold interface is excluded from possible structures with a high p-type SBH. With the T_4 structure, we obtained a SBH of 0.49 eV, which is 0.24 eV larger than the SBH of the type-B eightfold interface. This indicates the possibility that the atomic structure can cause the large p-type SBH at the type-B $CoSi_2$/Si(111) interface.

B. YSi_2/Si(111) interface

Since the atomic structure at the YSi_2/Si(111) interface has not yet been clarified, we evaluated it using the

surface structure of YSi_2. We assumed that the distance between the interfacial Y and Si layers [Fig. 2(d)] is the same as the distance between the Y and Si layers of bulk YSi_2. Including additional f orbitals, we used sixteen muffin-tin orbitals for Y atoms. Calculated p-type SBH's are 0.56 eV from the supercell's eigenvalue and Fermi energy, and 0.50 eV by the frozen potential method.

Figure 12 shows the LDOS of the YSi_2/Si(111) interface. The bulk Si DOS (dotted line) is adjusted to the eigenvalue E_v of the supercell. There are interface states in the Si band gap that appeared in the two-dimensional band (Fig. 2 in Ref. 8). Since the Y atom has only one d electron, a peak of d orbitals is above the Fermi energy. Bulk states of YSi_2 exist only near the K point around -9 eV in the two-dimensional band. This corresponds to the dip at -9 eV in the YSi_2 layer's LDOS. The energy state below the dip is formed by Si s orbitals. Just above the dip the Si s and p orbitals are hybridized. Near the interface the dip becomes smaller because the hybridized states have a lower energy. The interface affects the layered electronic structure in YSi_2.

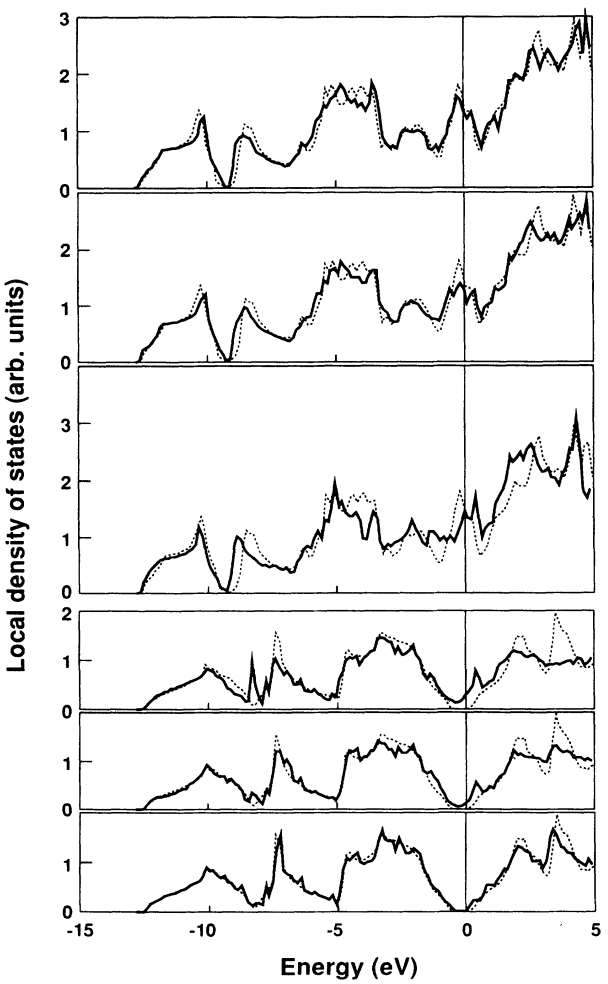

FIG. 12. Local density of states of the YSi_2/Si(111) interface. From top to bottom are the YSi_2 layer furthest from the interface, the second YSi_2 layer, the first YSi_2 layer, the first Si_2 layer, the second Si_2 layer, and the Si_2 layer furthest from the interface. Dotted lines are bulk densities of states of Si and YSi_2. Shaded areas are interface states. The zero energy point is the Fermi energy of the supercell.

From preliminary calculations without f orbitals for Y atom, we obtained an eigenvalue SBH of 0.44 eV, which is 0.12 eV lower than the result obtained with the f orbitals.[7] We calculated the DOS of bulk YSi_2 using LMTO-ASA with and without f orbitals for the Y atoms, and using FLAPW calculations (Fig. 13). The valence band width between the Fermi energy and the bottom of the valence band is 0.63 eV smaller with f orbitals than without f orbitals. The peak around -5 eV consists mainly of Si p orbitals, and the small peak around -2 eV consists mainly of Y d orbitals. These two peaks shift to higher energies when the f orbitals for Y atoms are included. The d-orbital states in the Y sphere (bold dotted lines) given by FLAPW are less than those given by LMTO-ASA, because FLAPW uses muffin-tin spheres while LMTO-ASA uses overlapping Wigner-Seitz spheres. The Si p states near -4 eV differ a little between the two methods: the Si p_z states (perpendicular to the layered plane) have a sharper peak in FLAPW. Since FLAPW includes the nonspherical potential in the atomic sphere, it describes the electronic structure of layered materials more accurately than LMTO-ASA. When the f orbitals are included in LMTO-ASA, the electronic structure, especially near the Fermi level, is closer to that given by FLAPW.

Since we thought of the possibility that the distance between the interface Si and Y layers [Fig. 2(d)] may be smaller than that in the bulk, we did the calculations with an interface Y-Si distance 0.1 Å smaller than the bulk value. In this structure the eigenvalue SBH was 0.66 eV and the band gap of the Si layer was 0.64 eV. The E_c of the Si layer was 0.02 eV lower than the Fermi energy of the supercell. Anyway, the 0.1 Å contraction of the interface Y-Si distance makes the SBH 0.1 eV higher. The SBH depends on the contraction in the same way as it depends on the f orbitals for Y atoms. In contrast to the YSi_2/Si(111) interface, the contraction of the interface Si-Si bond length at the type-A $NiSi_2$/Si(111) interface makes the SBH 0.05 eV lower.[18]

Figure 14 shows the difference in the number of electrons in each sphere at the interface and in the bulk for the supercell with and without the contraction of the interface distance. Because of the displacement of every other Si atom, one empty sphere enters at the YSi_2/Si(111) interface. Its radius and the number of electrons in it are given in Table VII. The interfacial Y sphere has about 0.6 less electrons. It seems that too many electrons left the interfacial Y atom. The interface empty sphere, however, has 0.46 electrons. Since the in-

TABLE VII. Sphere radii and number of electrons of the empty sphere located at the YSi_2/Si(111) interface

	Fixed	Contracted
Sphere radius (Å)	1.061	0.961
Number of electrons	0.461	0.357

terface empty sphere overlaps the interfacial Y sphere, a substantial number of electrons stay in the region near the interfacial Y atom. In the Si layer, spheres close to the interface have more electrons than in the bulk. This seems reasonable because the Si sphere of bulk YSi_2 has about 0.12 more electrons than that of bulk Si (Table I).

When the interface distance is contracted by 0.1 Å, the interface empty sphere is small and has about 0.36 electrons. In the Si layer, the two Si spheres close to the interface have less electrons than with the fixed distance. The total electron transfer from the YSi_2 layer to the Si layer is less with the interface contracted distance, although the p-type SBH is 0.1 eV higher.

At the $NiSi_2$/Si(111) interface, since the interface Si atoms are tetrahedrally bonded to their four nearest neighbors, the contraction of the interface distance does not change the direction of the interface Si-Si bond. At the YSi_2/Si(11) interface, the interfacial Y atom is at the H_3 site so that the direction of interfacial Y-Si bonding interaction is rotated 60° with respect to the interfacial Si back bonds. The contraction of the interface distance changes the direction of the interfacial Y-Si bonding interaction with respect to the interface plane. These structural differences cause the different SBH variations when the interface distance is contracted.

C. $NiSi_2$/Si(001) and $CoSi_2$/Si(001) interfaces

TEM lattice images suggested that the $NiSi_2$/Si(001) interface had a sixfold structure (Fig. 3). With a supercell containing six Si_2 and seven $NiSi_2$ layers, the sixfold structure's p-type SBH was −0.02 eV: the Fermi energy is lower than the valence band maximum of the Si layer (E_v). This is an unreasonable SBH. We previously reported that an incorrect fivefold model of the $CoSi_2$/Si(111) interface gives a negative SBH, although a correct eightfold model gives a positive and reasonable SBH.[6] Hence, we conclude that the sixfold model does not represent the $NiSi_2$/Si(001) interface. Another pos-

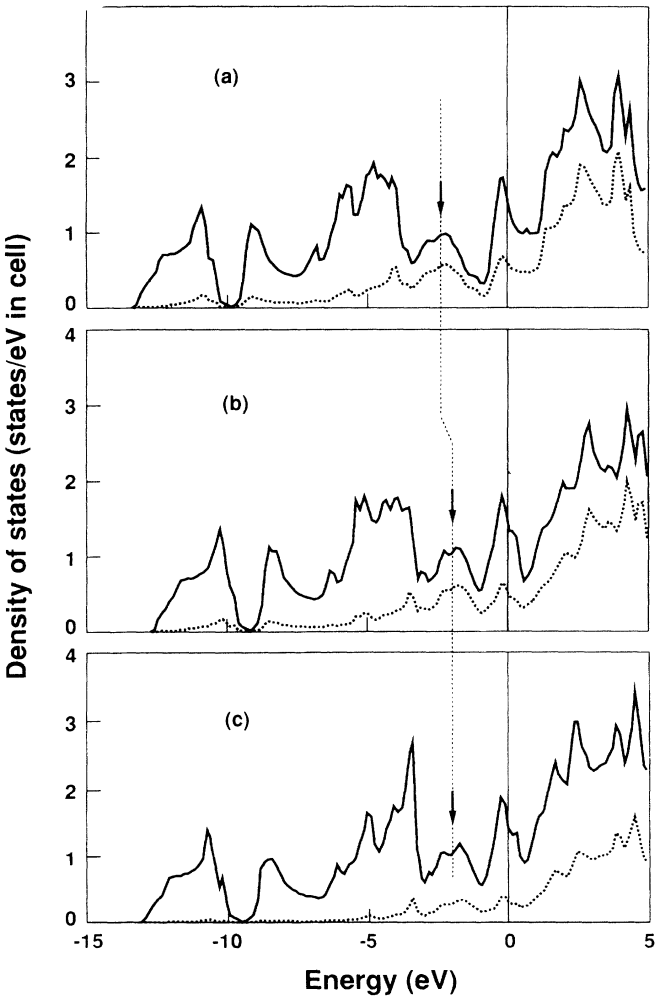

FIG. 13. Density of states of bulk YSi_2 calculated using LMTO-ASA for Y atoms (a) without f orbitals, (b) with f orbitals, and (c) density of states calculated by FLAPW. The dotted bold lines indicate Y d-orbital states in the Y sphere. The zero energy point is the Fermi energy. The arrows show the position of the small peak below the Fermi energy.

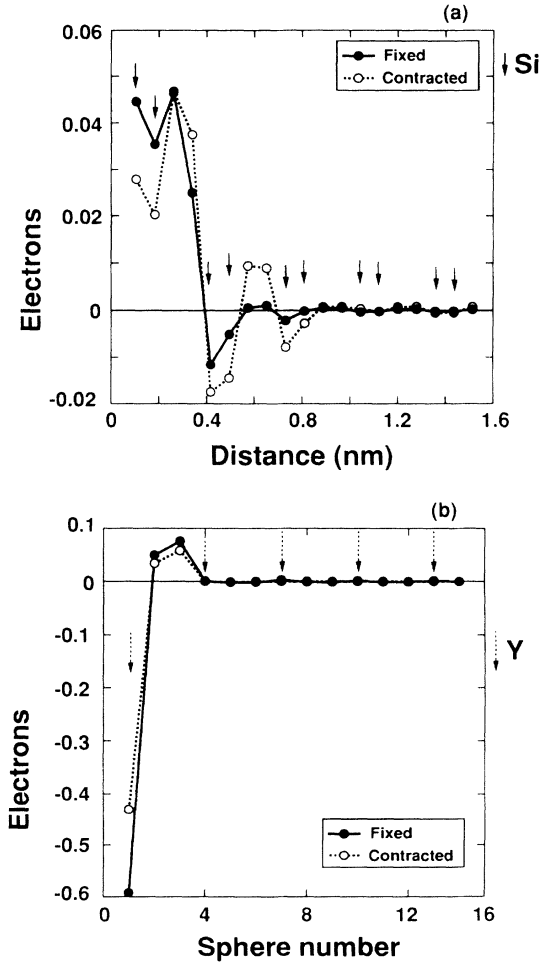

FIG. 14. Difference in the number of electrons in the spheres from the bulk values (a) in the Si layer and (b) in the YSi_2 layer. The interface is on the left. Arrows indicate atomic-sphere locations. In the YSi_2 layer, pairs of Si spheres are at the same distance from the interface.

sible structure for the $NiSi_2$/Si(001) interface is the eightfold model in which the interface Si atoms have two dangling bonds (Fig. 3). Since the $CoSi_2$/Si(111) interface has an eightfold structure, the eightfold model of (001) interface is one possible structure for the $CoSi_2$/Si(001) interface. So, we also studied the eightfold $CoSi_2$/Si(001) interface.

The supercell size affects the calculated SBH through the valence band width of each silicide and Si layer.[4] To compare the SBH's between the (001) and (111) interfaces, we used supercells with 11 Si_2 layers and 11 $NiSi_2$ or $CoSi_2$ layers for the eightfold (001) interface. Using the frozen potential method, we obtained p-type SBH's of 0.35 eV for the $NiSi_2$/Si(001) and 0.28 eV for the $CoSi_2$/Si(001). The frozen potential SBH's of the $NiSi_2$/Si(111) interface were 0.36 eV for type A and 0.19 eV for type B, which are obtained using the supercells with 12 Si_2 and 11 $NiSi_2$ layers.[4] The SBH of the eightfold $CoSi_2$/Si(111) interface is 0.29 eV for type A and 0.19 eV for type B (Table VI). The SBH's of the eightfold (001) interface are close to those of the type-A (111) structure at both the $NiSi_2$/Si and $CoSi_2$/Si interfaces.

Figure 15 shows the difference in number of electrons from the bulk value (Table I) at the eightfold $NiSi_2$/Si(001) and $CoSi_2$/Si(001) interfaces. No extra empty spheres enter at the interface. Since atoms are crowded at the eightfold (001) interface, spheres close to the interface have more electrons than in the bulk. Although the SBH differs by 0.07 eV between the $NiSi_2$/Si(001) and $CoSi_2$/Si(001) interfaces, the deviation of their electron distributions from that of the bulk is very similar.

The LDOS of the $NiSi_2$/Si(001) is very different from that of type-A $NiSi_2$/Si(111) interfaces.[5] At the (111) interface, the large peak of d electrons of the interface Ni

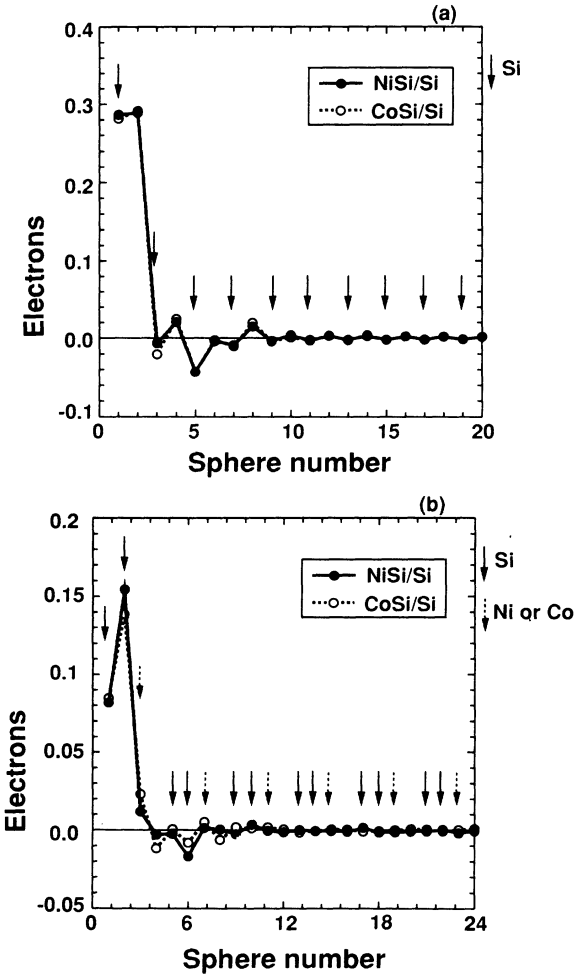

FIG. 15. Difference in the number of electrons in the spheres from the bulk values at the eightfold $NiSi_2$/Si(001) and $CoSi_2$/Si(001) interfaces (a) in the Si layer and (b) in the silicide layer. The interface is on the left-hand side. Arrows indicate atomic-sphere locations. In the Si layer, pairs consisting of a Si sphere and an empty sphere are at the same distance from the interface. In the silicide layer, pairs of Si spheres and pairs consisting of an empty sphere and a Ni or Co sphere are at the same distance from the interface.

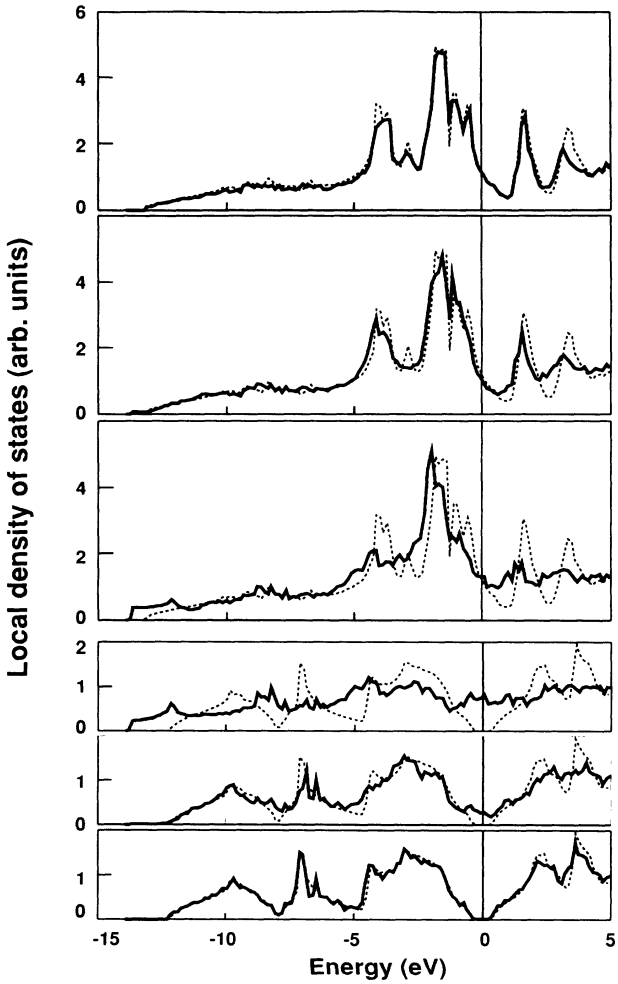

FIG. 16. Local densities of states of $CoSi_2$/Si(001) interfaces. From top to bottom are the $CoSi_2$ layer furthest from the interface, the second $CoSi_2$ layer, the first $CoSi_2$ layer, the first Si_2 layer, the second Si_2 layer, and the Si_2 layer furthest from the interface. Dotted lines are bulk densities of states of Si and $CoSi_2$. Shaded areas are interface states. The zero-energy point is the Fermi energy of the supercell.

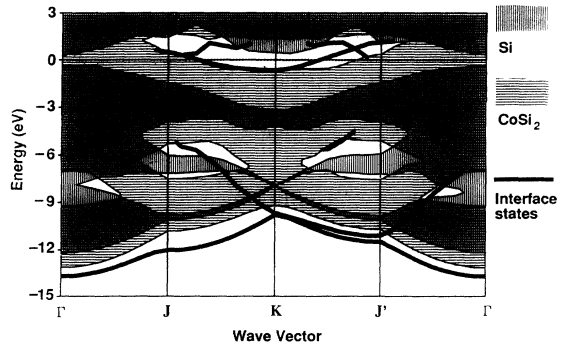

FIG. 17. Two-dimensional projected band structure of the eightfold $CoSi_2$/Si(001) interface obtained from the supercell eigenvalues. The zero energy point is the Fermi energy. Bold lines indicate the interface states that are localized near the interface.

atom is shifted to a higher energy; however, at the (001) interface, it remains at almost the same energy. At the (111) interface, the interface states originate from the interfacial Ni d orbital, while at the (001) interface they originate from the two dangling bonds of the interface Si atom. The LDOS of the eightfold $CoSi_2$/Si(001) interface (Fig. 16) resembles that of the eightfold $CoSi_2$/Si(111) interface. At the eightfold (001) interfaces, the interface Si atom has two dangling bonds, which produce the interface states both in the Si band gap and at the bottom of the valence band, in the same way as the eightfold $CoSi_2$/Si(111) interfaces whose interfacial Si atoms have one dangling bond.

Figure 17 shows a schematic two-dimensional band along the symmetry lines of the eightfold $CoSi_2$/Si(001) interface. It was obtained by examining the wave function weights of the eigenvalues. The zero energy is the Fermi level (E_f) of the supercell. Figure 17 reveals the lowering of the space-group symmetry of the supercell. The projected bulk band of Si and $CoSi_2$ is almost symmetrical about the vertical line at the K point, while the interface states are not symmetrical.

V. DISCUSSION

A. Calculated SBH's at (111) and (001) interfaces

We used two methods to obtain the SBH from the supercell calculation. The eigenvalue SBH is obtained from the Fermi energy (E_f) of the supercell and the eigenvalue of the valence band maximum (E_v) of the Si layer. E_v is distinguished from the large number of eigenvalues at the Γ point by examining the wave function character. By the frozen potential method, one-electron potentials of the silicide and Si layers farthest from the interface are cut from the self-consistent potential given by the supercell calculation, and exported to bulk band calculations, which yield the silicide Fermi energy (E'_f) and the Si valence band maximum (E'_v). In addition to these methods, the farthest Si layer's LDOS can be used to determine the Si valence band maximum.

Since we did not include the spin-orbit interaction, the E_v of bulk Si has threefold degeneracy. At the (111) interface, the supercell had $P\bar{3}m1$ (D^3_{3d}) symmetry, and the E_v is doubly degenerate and it appears at the Γ_3^+ point. In large supercells the E_v is easily distinguished by the wave function amplitude in the Si layer. At the (001) interface, the supercell had $Cmmm$ (D^{19}_{2h}) symmetry, and all eigenstates at the Γ point were single valued. From the eigenstates at the Γ point, we can identify the E_v of the Si layer and obtain the eigenvalue SBH with 11/11 supercells. However, the eigenvalue SBH was about 0.13 eV larger than the frozen potential SBH for both $NiSi_2$/Si(001) and $CoSi_2$/Si(001) interfaces, while the difference between these methods at the $NiSi_2$/Si(111) interface is about 0.03 eV with 11/12 supercells.[4] When we fitted the bulk Si DOS to the eigenvalue E_v, it deviated from the LDOS at the Si layer farthest from the (001) interface. The eigenvalue SBH at the (001) interface did not agree with the frozen potential SBH and the farthest Si layer's LDOS.

The projected Si region in the two-dimensional band at the $CoSi_2$/Si(001) interface (Fig. 17) consists of the eigenvalues whose wave function amplitude in the Si layer is above 40%. Among the Si band gap states near the Γ point, some eigenstates have wave functions with considerable amplitudes in the Si layers farther from the interface. These eigenstates have the character of the superlattice, not of the interface, because a periodic structure of the silicide and Si layers is assumed in the supercell calculation. Since Eq. (1) averages the wave function's fluctuations caused by the supercell geometry, the LDOS exhibits the character of the interface. At the (001) interface, the space symmetry of the supercell is lowered just by the interface structure, and the Si and silicide layers are more symmetrical than the interface structure (Fig. 17). The supercell must be larger than 11/11 supercells for the eigenvalue E_v to converge with respect to the supercell size. At the (111) interface, since the supercell keeps the symmetry of the Si and silicide layers, the eigenvalue SBH well agrees with LDOS in the farthest Si layer and is close to the frozen potential SBH with 11/12 supercells.

The frozen potential SBH is derived from the one-electron potentials in the Si and silicide layers farthest from the interface. Since the electron transfer occurs in the few layers near the interface, the one-electron potentials only vary near the interface (Fig. 3 in Ref. 5). Although the frozen potential SBH depends on the supercell size in the same way as the eigenvalue SBH, its fluctuation is smaller.[4] Before the eigenvalue SBH converges, the frozen potential method can be used to determine the SBH. We think that if the supercell is extremely large, the two methods will give the same SBH.

Considering the physical meaning of the band gap, we think that it is better to derive the SBH from the supercell's E_f and LDOS. The LDOS is locally defined and describes the detailed band structure, including the valence band width and interfacial gap states. The LDOS is also immune to the fluctuations caused by the supercell geometry. To obtain an accurate SBH from the LDOS,

TABLE VIII. Calculated Schottky-barrier height ($E_f - E_v$) of the supercells with 9 Si_2 and 8–10 silicide layers, and experimental values. Calculated values for the $NiSi_2$/Si(111) interfaces are taken from Ref. 4 and experimental values are taken from Refs. 15, 38, and 39 (in eV).

Structure	Calculations	Experiments
Type-A $NiSi_2$/Si(111)	0.32	0.47
Type-B $NiSi_2$/Si(111)	0.19	0.33
Type-B eightfold $CoSi_2$/Si(111)	0.25	0.42
H_3 YSi_2/Si(111)	0.56	0.73

however, we must use huge numbers of **k** points in the Brillouin zone.

To compare the theoretical and experimental results, we must consider the supercell size and the method used to derive the SBH. Table VIII summarizes the experimental SBH's and the eigenvalue SBH's for the silicide/Si(111) interface whose atomic structure is almost clarified. Since we obtained the calculated SBH's using the supercells with nine Si_2 layers and eight or ten silicide layers, these values may contain a convergence error of about 0.05 eV with respect to supercell size.[4] The calculated SBH's are about 0.15 eV smaller than the experimental values; however, the LDA calculations reflect the dependence of the SBH's on the interface atomic structure and type of metal silicide, although the LDA depresses the band gap of bulk Si to almost half of the experimental value. This is reasonable because the LDA calculation rigorously treats the electron distribution of the occupied states.

It is well known that the GW correction improves the band gap value of the semiconductor given by the LDA calculation.[51] Charlesworth, Godby, and Needs calculated the quasiparticle band structure of an Al/GaAs(110) interface using the GW self-energy operator.[52] They showed that the GW correction increases the p-type SBH by 0.1 eV and the n-type SBH by 0.4 eV compared with the LDA values. Although they did not deal with d electrons, their results also suggest that the LDA error reduces the calculated p-type SBH.

B. Electronic structure

The MIGS and interface states are peculiar to the interface. These electronic states introduced the Fermi level pinning model[10,11] and the concept of a "charge neutral level" into the study of metal-semiconductor interfaces.[53] When these models were proposed, the atomic and electronic structures of a real interface had not been clarified. Now we have a few examples whose atomic structure is almost clarified and whose electronic structure is given by the *ab initio* calculation. It is extremely important to examine the electronic structure of real metal-semiconductor interfaces.

The difference in the calculated SBH's of the two types of $NiSi_2$/Si(111) interfaces agrees well with the experimental value; however, the reasons for the difference are not yet clear. The interface state at the $NiSi_2$/Si(111) originates from the dangling d orbital of the interfacial Ni atom. The type-B interface state's lower energy was attributed to the different SBH's at the $NiSi_2$/Si(111) interfaces.[18,54] At the sevenfold $CoSi_2$/Si(111) interface, the dangling d orbital of the interfacial Co atom produces the interface states just at the Fermi level (Fig. 8). The p type SBH is 0.29 eV for type A and 0.07 eV for type-B. As with the $NiSi_2$/Si(111) interface, the interface state of type B is at a lower energy than that of type A with respect to the Si band. In the sevenfold structure the distance between the interfacial metal atom and the second Si atom on the Si side is shorter in type B than in type A. Bonding interactions between these atoms occurs in type B, therefore, the interface states of type B is at a lower energy than that of type A.

At the eightfold $CoSi_2$/Si(111) interface, the interface state originates from the dangling bond of the interfacial Si atom. The density of the interfacial gap states is, therefore, higher at the eightfold interface than at the sevenfold interface. As previously mentioned, at the type-A eightfold interface the distance between the interfacial Si atom and second Si atom in the Si layer is the same as bulk Si-Si distance and extra bonding interaction exists between them. Although the interface states and electron distributions of the sevenfold and eightfold interfaces differ significantly, the SBH of type B is lower than that of type A for both structures. The interface states do not seem to directly affect the SBH at the two types of sevenfold and eightfold interfaces.

The (111) and (001) $CoSi_2$/Si interfaces have different connections between the conduction band of the Si layer and the the $CoSi_2$ layer's band. The E_c of the Si layer is swallowed in the $CoSi_2$ band stomach (partial band gap) at the (111) interface (Fig. 5),[55] while the E_c at the Γ point continues into the $CoSi_2$ band at the (001) interface (Fig. 17). Hence, the (111) and (001) interfaces have different MIGS's near the E_c of the Si layer, but their SBH's are nearly the same. Since the two-dimensional projected band of metal silicides depends on the interface orientation, the MIGS's do not have an inherent distribution in the Si band gap.

Although the T_4 $CoSi_2$/Si(111) and H_3 YSi_2/Si(111) interfaces have a higher SBH than other interfaces, they have different electron distributions: the number of electrons on the Si side decreases at the T_4 $CoSi_2$/Si(111) and increases at the YSi_2/Si(111). The (001) and (111) type-A interfaces of $NiSi_2$/Si have nearly the same SBH's, but their electron distributions and interface states tremendously differ. The (001) and (111) type-A $CoSi_2$/Si interfaces also have almost the same SBH's despite the different electron distributions. The apparent difference of the interface electronic structures does not correspond to the SBH.

The electron transfer at the $NiSi_2$/Si and $CoSi_2$/Si interfaces is nearly the same for the same interface structures. The deviation of the number of electrons from the bulk values for the eightfold (001) interfaces (Fig. 15) and for each type of sevenfold (111) interface (compare Fig. 9 with Fig. 4 in Ref. 4) differs by no more than 0.02 electrons in any sphere, but the calculated SBH's differ by about 0.1 eV. The calculated SBH at the $NiSi_2$/Si(111)

interfaces fluctuated more than 0.1 eV depending on the supercell size. This was caused by a small difference in the electron distribution of up to 0.004 electrons in any spheres.[4] A small difference of the electron distribution is sufficient to change the SBH. Although the interface atomic structure causes different electron distributions and interface states at the metal-semiconductor interface, it does not alway change the SBH. This suggests that the SBH depends on specific characteristics of the interface atomic structure.

The interface states and MIGS's are not additional states, but are formed by states stolen from the Si valence and conduction band states. At every interface, the number of states in the Si layer decreases near -3 eV and increases in the Si band gap compared with that of the bulk Si (Fig. 5 in Ref. 7). Although the energy distribution of the interfacial gap states varies significantly with the interface atomic structure, that is, the interface bond configuration, the interfacial gap states are formed by the states stolen from the same energy range. Previously, from the cell size dependence of the SBH at the $NiSi_2$/Si(111) interface, we showed that the SBH depends on the valence band structures of both the Si and silicide layers, especially in the neighborhood of the Fermi energy and Si band gap, and the SBH does not depend much on the valence band bottom structures.[4] The energy states just below the Fermi level are critical to the SB formation.

The metal d electrons affect the SBH. At the YSi_2/Si(111) interface, the calculated SBH is 0.12 eV higher with the f orbitals for Y atoms than without the f orbitals. When the f orbitals are included, the small DOS peak around -2 eV formed mainly by Y d orbitals shifts to about 0.45 eV higher energy and is closer to the FLAPW result (Fig. 13). Hence, as the d electrons have higher energies, the p-type SBH is higher. The metal d electrons also affect the interface atomic structure. Using calculations on cluster modeling, van den Hoek, Ravenek, and Baerends found a simple picture explaining why the structures of the $CoSi_2$/Si(111) and $NiSi_2$/Si(111) interfaces differ.[56] They considered orbital overlap populations. At the eightfold interface, the metal d orbital and Si p_z orbital on the Si side form chemical bonds that have slightly more electrons at the $CoSi_2$/Si(111) interface than at the $NiSi_2$/Si(111) interface. At the sevenfold interface, the Si p_z orbitals on both the Si and silicide sides form chemical bonds that have slightly more electrons at the $NiSi_2$/Si(111) interface than at the $CoSi_2$/Si(111) interface. The major reason for this difference is that Ni atoms have one more d electron than Co atoms. Hence, the $CoSi_2$/Si(111) interface favors the eightfold structure and the $NiSi_2$/Si(111) interface favors the sevenfold structure. The interface atomic structure depends on the bulk properties of silicides, and the SBH depends on the interface atomic structure.

C. Interface structure and SBH

The type-B $CoSi_2$/Si(111) and $NiSi_2$/Si(111) interfaces have lower p-type SBH's than the type-A interfaces. The T_4 $CoSi_2$/Si(111) and H_3 YSi_2/Si(111) interfaces have larger SBH's than the type-A interfaces. These results suggest that twisted interfaces lower the SBH and interface bond bending raises the SBH. This feature is also supported by the calculations on the eightfold (001) interfaces, which do not have twisted structure or bond bending, and whose SBH's are close to those of the type-A (111) interfaces.

The $NiSi_2$/Si(001) interface formed by the conventional template technique has many ⟨111⟩ facets, which have the (111) type-A structure. The observed SBH at the $NiSi_2$/Si(001) interface has been attributed to the ⟨111⟩ facets. Our calculation shows that the eightfold $NiSi_2$/Si(001) interface has almost the same SBH as the (111) type-A interface. We propose that the observed SBH at the (001) interface is attributed not only to the ⟨111⟩ facets and but also to the eightfold (001) structure. However, since interfacial Si atoms at the eightfold (001) interface have two dangling bonds, we suppose that during the interface formation, the dangling bonds form bonding states with each other or with other atoms, and hence the (001) interface probably contains other atomic structures.

It is well known that the Si(001) surface consists of dimerized pairs of atoms with 2×1 symmetry. Similar reconstructions are also observed at buried metal-semiconductor interfaces.[57] Loretto, Gibson, and Yalisove found separate 2×1 and 1×2 domains at a $CoSi_2$/Si(001) interface which was formed by depositing a few monolayers of either pure Co or Co and Si at room temperature and then annealed to $\sim500\,^{\circ}C$.[58] At the $NiSi_2$/Si(001) interface, Tung *et al.* found that high-temperature ($>700\,^{\circ}C$) annealing eliminated the ⟨111⟩ facets, and formed the planar $NiSi_2$/Si(001) interface.[44] This planar interface has an extraordinarily high p-type SBH, and evidence of 1×2 reconstructed regions suggests that it has an inhomogeneous atomic structure. The interfacial reconstruction is more clearly seen with the $CoSi_2$/Si(001) than with the $NiSi_2$/Si(001), possibly because of the interface stability. The difference between the interface energies is given accurately even by LMTO-ASA, because the calculation conditions are the same as for the eightfold (001) interfaces. The interface energy at the $CoSi_2$/Si(001) was 0.05 eV higher than at the $NiSi_2$/Si(001): the eightfold 1×1 structure is more unfavorable at the $CoSi_2$/Si(001) than at the $NiSi_2$/Si(001).

Sullivan *et al.* reported an extremely high p-type SBH for the type-B $CoSi_2$/Si(111) interface. To study possible interface structures, we examined the sevenfold and T_4 interfaces. The calculated SBH for the type-B sevenfold interface is 0.07 eV, which is smaller than that of the type-B eightfold interface. Hence, the sevenfold interface is not a possible structure. With the T_4 structure, we demonstrate the possibility that the atomic structure can cause the large p-type SBH at the type-B $CoSi_2$/Si(111) interface. However, since the electron distribution at the T_4 structure deviates significantly from the bulk, we consider that the T_4 structure is not a possible structure.[59] At the $NiSi_2$/Si(001) and $CoSi_2$/Si(111) interfaces with high p-type SBH's, experimental evidence indicates that the reconstructed regions exist at the buried interface. Although these interface structures have not yet been

clarified, we speculate that the reconstructed structure causes bond bending at the interface, and that this increases the p-type SBH.

In our calculations, we only studied the metal silicide/Si interfaces with 1×1 symmetry. So, the structure has a perfect periodicity along the interface, and the direction of the interfacial bonding interaction is perfectly ordered. The calculation with an artificial interface atomic structure gives various SBH's, which are significantly different from the experimental SBH.[60] The real interface is always formed according to energetics, which are comparable to the thermal energy and are a very small energy for the LDA calculation. Metal-semiconductor interfaces usually have complicated atomic structures and the directions of the interfacial bonding interactions are probably disordered. Since the SBH depends on the supercell size, the SBH is influenced by the number of atoms connected by the bonding interaction, especially, the interaction between the atomic orbitals near the Fermi level. We suppose that these interactions dominate the SB formation in the absence of the ordered interface atomic structure.

When the interface consists of small domains with different atomic structures, it is difficult to observe local SBH's even by ballistic electron emission microscopy.[61] To study the relationship between the SBH and interface structure, a large area of highly perfect interfaces is required because the potential pinch-off near the interface hides the local SBH inhomogeneity.[62,63] Studies using carefully controlled formation conditions have shown the structure dependence of the SBH for other metal-semiconductor interfaces: Pb/Si(111) interfaces[64,65] and metal/GaAs(001).[66,67] It is certain that the SBH depends on the interface atomic structure; however, the differences in the interface structure are not sufficient to change the SBH. Using ballistic electron emission spectroscopy and a highly doped substrate, Palm, Arbes, and Schulz made the local SBH fluctuations directly visible at the Au/Si interface.[68] They observed SBH fluctuations at the Au/Si(001) interface but did not at the Au/Si(111) interface. The p-type SBH is higher in randomly distributed areas than the average SBH at the Au/Si(001) interface. The cause has not been determined, but since the 2×1 reconstructed structure is more favorable at the (001) interface than the (111) interface, we expect interfacial reconstruction to raise the p-type SBH in the same way as at the planar $NiSi_2$/Si(001) interface.

VI. SUMMARY

Using LMTO-ASA, we studied the electronic structure of $CoSi_2$/Si(111), YSi_2/Si(111), $NiSi_2$/Si(001), and $CoSi_2$/Si(001) interfaces. We determined atomic-sphere radii based on the more accurate FLAPW calculation on bulk silicides. To overcome the lack of periodicity perpendicular to the interface, we used large supercells with 9 Si_2 and 8–10 silicide ($CoSi_2$, YSi_2) layers for the (111) interface, and with 11 Si_2 and 11 silicide ($NiSi_2$, $CoSi_2$) layers for the (001) interface. Considering the cell size dependence and the method of deriving SBH from the supercell calculation, we showed that the LDA calculation gives a p-type SBH about 0.15 eV lower than the experimental value when the correct interface structure is used.

The electronic character of bulk silicide affects the interface atomic structure and the SB formation. The p-type SBH tends to increase with the energy of the metal d-electron. The interface electronic structure, such as interface states and electron distribution, directly depends on the interface atomic structure; by contrast, the calculated SBH does not always depend on the interface structure. The disturbance caused by the interface structure is dielectrically screened out within two or three layers. The remaining effect of the interfacial bonding interaction, especially its direction at the metal-semiconductor interface in ordered atomic structures, affects the SBH.

ACKNOWLEDGMENTS

We would like to thank Dr. R. R. Tung for valuable discussions and for sending us his results prior to publication. We are also grateful to H. Ishikawa, T. Itoh, and N. Nakayama for their encouragement.

[1] P. Hohenberg and W. Kohn, Phys. Rev. **136**, B864 (1964).
[2] W. Kohn and L. J. Sham, Phys. Rev. **140**, A1133 (1965).
[3] H. Fujitani and S. Asano, Phys. Rev. B **40**, 8357 (1989); Surf. Sci. **268**, 265 (1992).
[4] H. Fujitani and S. Asano, Phys. Rev. B **42**, 1696 (1990).
[5] H. Fujitani and S. Asano, J. Phys. Soc. Jpn. **60**, 2526 (1991).
[6] H. Fujitani and S. Asano, Appl. Surf. Sci. **41/42**, 164 (1989).
[7] H. Fujitani and S. Asano, Mat. Res. Soc. Symp. Proc. **193**, 77 (1990).
[8] H. Fujitani and S. Asano, Appl. Surf. Sci. **56–58**, 408 (1992).
[9] W. Schottky, Z. Phys. **118**, 539 (1942).
[10] J. Badeen, Phys. Rev. **71**, 717 (1947).
[11] V. Heine, Phys. Rev. **138**, 1689 (1965).
[12] S. G. Louie and M. L. Cohen, Phys. Rev. B **13**, 2461 (1976).
[13] C. Tejedor, F. Flores, and E. Louis, J. Phys. C **10**, 2163 (1977).
[14] J. Tersoff, Phys. Rev. Lett. **52**, 465 (1984).
[15] R. T. Tung, Phys. Rev. Lett. **52**, 461 (1984).
[16] J. M. Gibson, R. T. Tung, and J. M. Poate, in *Defects in Semiconductors II*, Proceedings of the Materials Research Society Symposium, No. 14, Boston, 1982, edited by S. Mahajan and James W. Corbett (North-Holland, New York, 1983), p. 395.
[17] H. Fujitani and S. Asano, J. Phys. Soc. Jpn. **57**, 2253 (1988).
[18] G. P. Das, P. Blöchl, N. E. Christensen, and O. K. Andersen, in *Metallization and Metal-Semiconductor Interfaces*,

edited by I. P. Batra (Plenum, New York, 1988); G. P. Das, P. Blöchl, O. K. Andersen, N. E. Christensen, and O. Gunnarsson, Phys. Rev. Lett. **63**, 1168 (1989).
[19]D. Cherns, G. R. Anstís, J. L. Hutchinson, and J. C. H. Spence, Philos. Mag. A **46**, 849 (1982).
[20]J. M. Gibson, J. C. Bean, J. M. Poate, and R. T. Tung, Appl. Phys. Lett. **41**, 818 (1982).
[21]J. Zegenhagen, K. G. Huang, B. G. Hunt, and L. J. Schowalter, Appl. Phys. Lett. **51**, 1176 (1987).
[22]E. J. van Loenen, J. W. M. Frenken, J. F. van der Veen, and S. Valeri, Phys. Rev. Lett. **54**, 827 (1985).
[23]D. R. Hamann, Phys. Rev. Lett. **60**, 313 (1988).
[24]N. V. Rees and C. C. Matthai, J. Phys. C **21**, L981 (1988).
[25]M. L. Cohen and J. R. Chelikowsky, *Electronic Structure and Optical Properties of Semiconductors* (Springer-Verlag, New York, 1988).
[26]J. Tersoff and D. R. Hamann, Phys. Rev. B **28**, 1168 (1983).
[27]F. Hellman and R. T. Tung, Phys. Rev. B **37**, 10 786 (1988).
[28]J. Vrijmoeth, A. G. Schins, and J. F. van der Veen, Phys. Rev. B **40**, 3121 (1989).
[29]J. Vrijmoeth, S. Zaima, E. Vlieg, and J. W. M. Frenken, Phys. Rev. B **45**, 6700 (1992).
[30]A. Santaniello, P. DePadova, X. Jin, D. Chandesris, and G. Rossi, J. Vac. Sci. Technol. B **7**, 1017 (1989).
[31]L. Haderbache, P. Wetzel, C. Pirri, J. C. Peruchetti, D. Bolmont, and G. Gewinner, Phys. Rev. B **39**, 12 704 (1989).
[32]R. T. Tung, A. F. J. Levi, and J. M. Gibson, Appl. Phys. Lett. **48**, 635 (1986).
[33]R. T. Tung and J. L. Batstone, Appl. Phys. Lett. **52**, 1611 (1988).
[34]R. T. Tung and J. L. Batstone, Appl. Phys. Lett. **52**, 648 (1988).
[35]R. T. Tung, J. Vac. Sci. Technol. **A7**, 598 (1989).
[36]R. T. Tung, J. Vac. Sci. Technol. **2**, 465 (1984).
[37]E. Rosencher, S. Delage, and F. Arnaud D'Avitaya, J. Vac. Sci. Technol. **B3**, 762 (1985).
[38]J. P. Sullivan, R. T. Tung, D. J. Eaglesham, F. Schrey, and W. R. Graham, J. Vac. Sci. Technol. **11**, 1564 (1993).
[39]K. N. Tu, R. D. Thompson, and B. Y. Tsaur, Appl. Phys. Lett. **38**, 626 (1981).
[40]J. A. Knapp and S. T. Picraux, Appl. Phys. Lett. **48**, 466 (1986).
[41]M. P. Siegal, J. J. Santiago, and W. R. Graham, Mat. Res. Soc. Symp. Proc. **198**, 589 (1990).
[42]R. Baptist, S. Ferrer, G. Grenet, and H. C. Poon, Phys. Rev. Lett. **64**, 311 (1990).
[43]D. Cherns, C. J. D. Hetherington, and C. J. Humphreys, Philos. Mag. A **49**, 165 (1984).
[44]R. T. Tung, A. F. J. Levi, J. P. Sullivan, and F. Schrey, Phys. Rev. Lett. **66**, 72 (1991).
[45]J. F. Janak, V. L. Moruzzi, and A. R. Williams, Phys. Rev. B **12**, 1257 (1975).
[46]O. K. Andersen, Phys. Rev. B **12**, 3060 (1975); O. K. Andersen, O. Jepsen, and D. Glötzel, in *Highlights of Condensed Matter Theory*, edited by F. Bassani, F. Fumi, and M. P. Tosi (North-Holland, Amsterdam, 1985), p. 59; O. K. Andersen, O. Jepsen, and M. Sob, in *Electronic Band Structure and its Applications*, edited by M. Yussouff (Springer-Verlag, Heidelberg, 1987).
[47]E. Wimmer, H. Krakauer, M. Weinert, and A. J. Freeman, Phys. Rev. B **24**, 864 (1981).
[48]E. Vlieg, A. E. M. J. Fischer, J. F. van der Veen, B. N. Dev, and G. Materlik, Surf. Sci. **178**, 36 (1986).
[49]J. Zegenhagen, K. G. Huang, W. M. Gibson, B. D. Hunt, and L. J. Schowalter, Phys. Rev. B **39**, 10 254 (1989).
[50]F. Flores and J. Ortega, Appl. Surf. Sci. **56–58**, 301 (1992).
[51]M. Hybersten and S. G. Louie, Phys. Rev. B **34**, 5390 (1986).
[52]J. P. A. Charlesworth, R. W. Godby, and R. J. Needs, Phys. Rev. Lett. **70**, 1685 (1993).
[53]For a review of the metal-semiconductor interface, refer, for example, to F. Flores and C. Tejedor, J. Phys. C **20**, 145 (1987).
[54]S. Ossicini, O. Bisi, and C. M. Bertoni, Phys. Rev. B **42**, 5735 (1990).
[55]L. F. Mattheiss and D. R. Hamann, Phys. Rev. B **37**, 10 623 (1988).
[56]P. J. van den Hoek, W. Ravenek, and E. J. Baerends, Phys. Rev. Lett. **60**, 1743 (1988); Surf. Sci. **205**, 549 (1988).
[57]K. Akimoto, I. Hirosawa, J. Mizuki, S. Fujieda, Y. Matsumoto, and J. Matsui, Jpn. J. Appl. Phys. **27**, L1401 (1988).
[58]D. Loretto, J. M. Gibson, and S. M. Yalisove, Phys. Rev. Lett. **63**, 298 (1989).
[59]The interface energy of the T_4 structure obtained by our FLAPW calculations is more than 1 eV when the interfacial Co-Si distance is 2.3–3.2 Å, while the eightfold type-B interface has an interface energy of 0.53 eV (Ref. 23).
[60]M. van Schilfgaarde and N. Newman, Phys. Rev. Lett. **65**, 2728 (1990).
[61]Y. Hasegawa, Y. Kuk, R. T. Tung, P. J. Silverman, and T. Sakurai, J. Vac. Sci. Technol. B **9**, 578 (1991).
[62]J. L. Freeouf, T. N. Jackson, S. E. Laux, and J. M. Woodall, J. Vac. Sci. Technol. **21**, 570 (1982).
[63]T. Tung, Phys. Rev. B **45**, 13 509 (1992).
[64]G. Le Lay, K. Hricovini, and J. E. Bonnet, Appl. Surf. Sci. **41/42**, 25 (1989).
[65]D. R. Heslinga, H. H. Weitering, D. P. van der Werf, T. M. Klapwijk, and T. Hibma, Phys. Rev. Lett. **64**, 1589 (1990).
[66]K. Hirose, K. Akimoto, I. Hirosawa, J. Mizuki, T. Mizutani, and J. Matsui, Phys. Rev. B **43**, 4538 (1991).
[67]S. Chang, L. J. Brillson, Y. J. Kime, D. S. Rioux, P. D. Kirchner, G. D. Pettit, and J. M. Woodall, Phys. Rev. Lett. **64**, 2551 (1990).
[68]H. Palm, M. Arbes, and M. Schulz, Phys. Rev. Lett. **71**, 2224 (1993).

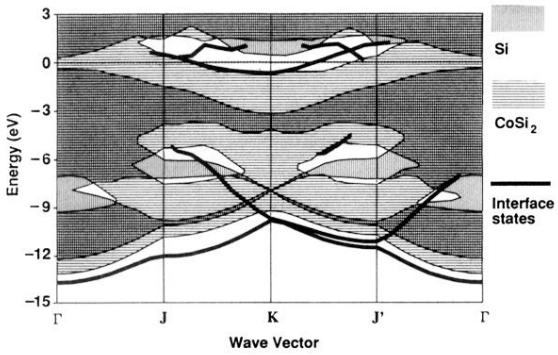

FIG. 17. Two-dimensional projected band structure of the eightfold $CoSi_2/Si(001)$ interface obtained from the supercell eigenvalues. The zero energy point is the Fermi energy. Bold lines indicate the interface states that are localized near the interface.

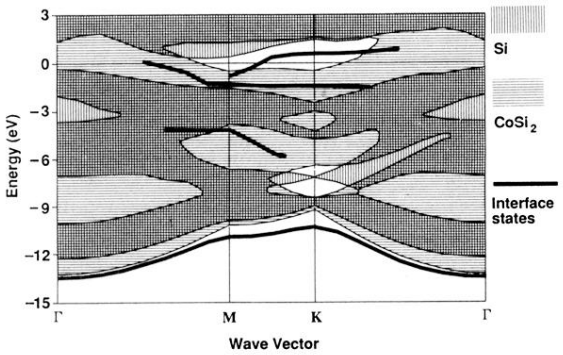

FIG. 5. Two-dimensional projected band structure of the type-A $CoSi_2/Si(111)$ interface obtained from the supercell calculation. The zero energy point is the Fermi energy. Bold lines indicate the interface states that are localized near the interface.